© 2020. Published by The Company of Biologists Ltd | Journal of Cell Science (2020) 133, jcs238337. doi:10.1242/jcs.238337

RESEARCH ARTICLE

SPECIAL ISSUE: CELL BIOLOGY OF THE IMMUNE SYSTEM

Vav2 lacks Ca^{2+} entry-promoting scaffolding functions unique to Vav1 and inhibits T cell activation via Cdc42

Michael A. Fray[1], John C. Charpentier[2], Nicholas R. Sylvain[1], Maria-Cristina Seminario[1] and Stephen C. Bunnell[1,*]

ABSTRACT

Vav family guanine nucleotide exchange factors (GEFs) are essential regulators of immune function. Despite their structural similarity, Vav1 promotes and Vav2 opposes T cell receptor (TCR)-induced Ca^{2+} entry. By using a Vav1-deficient Jurkat T cell line, we find that Vav1 facilitates Ca^{2+} entry via non-catalytic scaffolding functions that are encoded by the catalytic core of Vav1 and flanking linker regions. We implicate, in this scaffolding function, a previously undescribed polybasic motif that is strictly conserved in Vav1 and absent from Vav2 in tetrapods. Conversely, the catalytic activity of Vav2 contributes to the suppression of TCR-mediated Ca^{2+} entry. By performing an *in vivo* 'GEF trapping' assay in intact cells, we demonstrate that Cdc42 interacts with the catalytic surface of Vav2 but not Vav1, and that Vav1 discriminates Cdc42 from Rac1 via F56 (W56 in Rac1). Finally, the Cdc42-specific inhibitor ZCL278 and the shRNA-mediated suppression of Cdc42 each prevent the inhibition of TCR-induced Ca^{2+} entry by Vav2. These findings define stark differences in the functions of Vav1 and Vav2, and provide an explanation for the differential usage of these Vav isoforms by immune subpopulations.

KEY WORDS: Vav2, Vav1, T cell, Cdc42, Rac1, Calcium, Ca^{2+}

INTRODUCTION

The Vav family is a group of paralogous proto-oncoproteins that act as guanine nucleotide exchange factors (GEFs) for Rho family GTPases (Bustelo, 2012, 2014). The three Vav proteins are unique among the Rho GEFs in possessing a Src homology 2 (SH2) domain, which enables their participation in diverse tyrosine kinase-dependent signaling pathways. Through their catalytic and scaffolding functions, Vav proteins influence the signals initiated by receptor tyrosine kinases, immunoreceptors, integrins and cytokine receptors, and impact the development, growth and activation of diverse immune and non-immune cells.

Vav1 is the isoform that is most restricted to the hematopoietic system and is most highly expressed throughout the hematopoietic system. In contrast, Vav2 and Vav3 are more broadly expressed and have important roles in non-immune tissues (Tedford et al., 2001; Turner and Billadeau, 2002; Fujikawa et al., 2003). Vav1 knockouts have dramatic effects on T cell development and activation. These defects are exacerbated by the loss of Vav3 but are virtually unaffected by the further loss of Vav2. In contrast, Vav1 and Vav2 both play important roles in B cell development and activation, with double knockouts exhibiting more profound abnormalities than either individual knockout. At one level, these patterns of redundancy may simply reflect the expression of Vav isoforms in these tissues. However, the Vav isoforms play distinct roles in immune cells. In particular, Vav1 is required for the initiation of optimal Ca^{2+} elevations downstream of the T cell receptor (TCR) and plays a crucial role in the activation of the nuclear factor of activated T-cells (NF-AT) proteins (Fischer et al., 1995). Vav3, while not required for TCR-dependent Ca^{2+} and NF-AT responses, enables residual Ca^{2+} and NF-AT responses in the absence of Vav1 (Fujikawa et al., 2003; Charvet et al., 2005). In sharp contrast, the heterologous expression Vav2 in T cells potently inhibits the entry of Ca^{2+} and the activation of NF-AT in T cells (Doody et al., 2000; Tartare-Deckert et al., 2001). This suppressive effect does not reflect a generalized inhibitory function, as Vav2 enhances both Ca^{2+} entry and the activation of NF-AT downstream of the B cell receptor (BCR) (Fujikawa et al., 2003). Thus, Vav1 and Vav2 must possess distinct functions that are modulated by the cellular context to determine the ultimate outcome of Vav2 signaling. However, very little is known about the molecular bases of differences in Vav isoform function.

The overall architecture of the Vav proteins arose early in metazoan evolution (Fig. 1A) (Bustelo, 2014). The catalytic core is flanked at the N-terminus by a calponin homology (CH) domain and a regulatory linker that is rich in acidic amino acids. In the resting state, this linker occludes the catalytic surface and is stabilized in place via interactions involving the CH domain and the catalytic core (Aghazadeh et al., 2000; Yu et al., 2010). Vav GEFs also incorporate a C-terminal adaptor region that contains an SH2 domain and two Src homology 3 (SH3) domains. This module also folds back onto the catalytic core to restrict the basal activity of the central GEF module (Barreira et al., 2014). Deletions that truncate the N-terminal CH domain or the C-terminal SH3 domain constitutively activate Vav proteins and contribute to oncogenic transformation via the uncontrolled activation of Rho GTPases (Katzav, 2007; Abate et al., 2017; Kogure and Kataoka, 2017). Under normal stimulatory conditions, the C-terminal adaptor module recruits Vav proteins into tyrosine kinase-coupled signaling complexes and facilitates the tyrosine phosphorylation of crucial tyrosine residues in the acidic linker region, the C1 domain and the C-terminus of the protein (Barreira et al., 2014, 2018). These phosphorylations release the inhibitory interactions mediated by the N- and C-terminal regions and enable GEF activity. Although Vav1, Vav2 and Vav3 all activate Rac1, and to a lesser degree RhoA, the full spectrum of Rho GTPases targeted by these GEFs is less well-established. In particular, most studies agree that Vav1 and Vav3 are poor Cdc42 GEFs, while studies that have

[1]Program in Immunology, Department of Immunology, Tufts University School of Medicine, Boston, MA 02111, USA. [2]Department of Biology, University of Massachusetts Boston, Boston, MA 02125, USA.

*Author for correspondence (stephen.bunnell@tufts.edu)

M.A.F., 0000-0001-8388-1875; J.C.C., 0000-0001-9488-8239; M.-C.S., 0000-0003-0762-8661; S.C.B., 0000-0001-6887-0828

Received 20 August 2019; Accepted 6 January 2020

Journal of Cell Science (2020) 133, jcs238337. doi:10.1242/jcs.238337

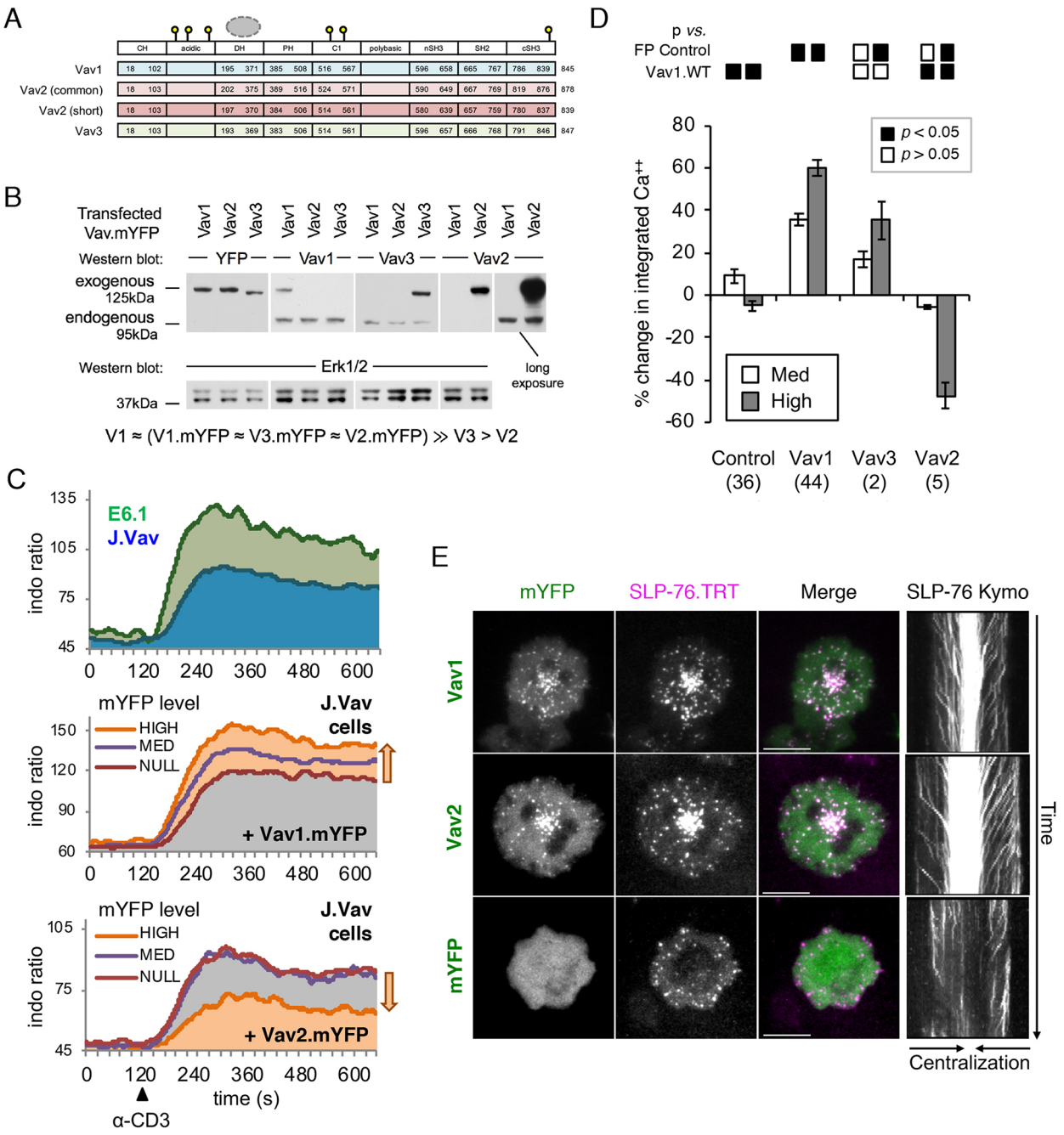

Fig. 1. See next page for legend.

addressed the activity of Vav2 towards Cdc42 are divided on the topic (Bustelo, 2014).

In addition to their roles as GEFs, the Vav proteins function as scaffolding proteins. In activated T cells, Vav1 enters the SLP-76 (also known as LCP2)-containing microclusters, which are dynamically assembled in response to receptor engagement (Bunnell, 2010). These structures are signaling hubs that incorporate multiple proteins with crucial roles in T cell activation, including phospholipase Cγ1 (PLCγ1). The loss of Vav1 destabilizes these structures and impairs multiple downstream signals, including TCR-initiated increases in PLCγ1 phosphorylation and cytoplasmic Ca^{2+} (Fischer et al., 1995; Turner et al., 1997; Reynolds et al., 2002). Catalytically inactive forms of Vav1 effectively reconstitute microcluster stability and TCR-mediated Ca^{2+} entry, but do not fully rescue the developmental and functional defects associated with the loss of Vav1 (Kuhne et al., 2000; Miletic et al., 2009; Saveliev et al., 2009; Sylvain et al., 2011). In addition to the C-terminal adaptor region, these scaffolding functions require poorly characterized elements within the N-terminal portion of Vav1, including the CH domain and the catalytic core itself (Billadeau et al., 2000; Sylvain et al., 2011).

To understand how Vav1 and Vav2 differentially influence Ca^{2+} signaling downstream of the TCR, we generated chimeric proteins in which critical functional domains were exchanged and expressed these chimeras in a Vav1-deficient T cell line. We identified two fundamental features that drive the differential behaviors of Vav1 and Vav2 in T cells. First, we identified a conserved polybasic motif that is

Journal of Cell Science (2020) 133, jcs238337. doi:10.1242/jcs.238337

Fig. 1. Vav2 inhibits Ca^{2+} influx in Jurkat T cells. (A) The domain structures and predicted domain boundaries for the Vav proteins are depicted. Conserved regulatory tyrosine phosphorylation sites (yellow circles) and the GTPase binding site (grey circle) are highlighted. Throughout these studies we employ the longer isoform of Vav2. All Vav chimeras are tagged at the C-terminus with fluorescent proteins (not shown). (B) Transitive western blots reveal the relative abundances of endogenous Vav1, Vav2 and Vav3 in the parental E6.1 Jurkat line by comparison with mYFP-tagged exogenous constructs expressed at similar levels. Each vertical panel is from a different gel with the same lysates. The loading controls are from the same lanes as the panels above them. Representative of two experiments. (C) Representative Ca^{2+} responses in Jurkat cells. Top panel, parental E6.1 Jurkat cells (green shading) and Vav1-deficient J.Vav1 cells (blue shading) were loaded with Indo-1. Ca^{2+} responses were continuously monitored by flow cytometry. Cells were stimulated at 2 min using 30 ng ml^{-1} OKT3 (anti-CD3ε). Mean Indo-1 ratios are shown. Bottom panels, J.Vav1 cells expressing mYFP-tagged Vav1 or Vav2 (Vav1.mYFP and Vav2.mYFP) were assessed for Ca^{2+} influx as above. Responses are presented for populations isolated from the bulk by gating for distinct levels of mYFP fluorescence. Responses of non-transfected cells (NULL, brown line, gray shading), moderate expression (MED, purple line) and high expression (HIGH, orange line, orange shading) are superimposed. Arrows on the right emphasize the shift in Ca^{2+} entry observed between non-expressing and highly expressing cells in the same tube. (D) Quantification of Ca^{2+} influx data for the indicated mYFP-tagged Vav chimeras. Experiments were performed as in C. The percentage changes in the integrated Ca^{2+} responses of the moderate and high mYFP-expressing populations were calculated relative to non-transfected, non-expressing cells within the same sample. Graphs depict the cumulative mean±s.e.m. for all salient experiments. The number of independent replicates is shown in parentheses. Small boxes above each chart depict *P*-values for statistical comparisons between cells expressing matched levels of the chimeras indicated directly below and at left. (E) Vav1-deficient Jurkat cells stably expressing TRT-tagged SLP-76 (J.Vav1.SLP.TRT) were transfected with vectors encoding Vav1.mYFP, Vav2.mYFP or mYFP. Cells were plated on glass surfaces coated with anti-CD3ε (10 µg ml^{-1} OKT3) and imaged continuously for 5 min. Selected still images are shown on the left, with the merge pseudocoloring the mYFP chimera in green and the SLP-76 chimera in magenta. At the right, kymographs depict the movement of SLP-76 microclusters through a narrow cross-section of the cell over time. Representative images from two or more experiments are shown. Scale bars: 10 µm and apply to all panels. Kymographs span the full 5 min imaging period.

found in Vav1, but not Vav2, and that is required for Vav1 to enhance TCR-induced Ca^{2+} signals via non-catalytic mechanisms. In addition, we determined that the catalytic activity of Vav2 is distinct from that of Vav1 and is responsible for the active suppression of Ca^{2+} signals initiated by the TCR. By performing a novel 'GEF trap' assay, we demonstrated that Cdc42 is recruited to the catalytic surface of Vav2, but is excluded from Vav1. Using a constitutively active form of Cdc42 in conjunction with a small-molecule inhibitor of Cdc42 activation, we confirmed that Vav2 suppresses TCR-induced Ca^{2+} responses via Cdc42. Finally, we established that the suppression of Cdc42 prevents the inhibition of TCR-initiated Ca^{2+} responses by Vav2. These findings raise the possibility that the distinctive aspects of Vav function could be independently targeted in order to achieve more-selective cancer therapies and immunotherapies.

RESULTS

Vav2 inhibits TCR-induced Ca^{2+} responses in Jurkat T cells

To evaluate the abilities of fluorescently tagged variants of all three Vav proteins to support TCR-mediated Ca^{2+} entry, we generated Vav chimeras tagged with mYFP and expressed these proteins at levels comparable to endogenous Vav1 in wild-type Jurkat leukemic T cells (Fig. 1A). Transitive western blotting confirmed that endogenous Vav2 and Vav3 are present in these cells, but are ∼50-fold (Vav2) and ∼20-fold (Vav3) less-abundant than Vav1 (Fig. 1B). Based on these data, we identified mYFP fluorescence intensities that correspond to expression at levels comparable to Vav1 in wild-type Jurkat cells. When expressed at these levels in a Vav1-deficient Jurkat-derived line (J.Vav1), the Vav1–mYFP chimera augments, but does not fully restore, TCR-mediated Ca^{2+} entry (Fig. 1C, middle, 'MED'; Fig. 1D). Higher levels of Vav1 chimera are required to support normal TCR-initiated Ca^{2+} responses in J.Vav1 cells (Fig. 1C, middle, 'HIGH', versus upper 'E6.1'; Fig. 1D). Vav3 chimeras also enhance Ca^{2+} entry, although they are less potent than Vav1 when expressed at matched levels (Fig. 1D). This is consistent with the observation that Vav3 supports the residual NF-AT responses of TCR-stimulated J.Vav1 cells (Cao et al., 2002; Charvet et al., 2005). In contrast to Vav1 and Vav3, and consistent with prior reports, Vav2 antagonizes TCR-mediated Ca^{2+} entry (Fig. 1C, lower; Fig. 1D) (Doody et al., 2000; Tartare-Deckert et al., 2001). This effect only becomes significant at the higher level of expression, when the Vav2 chimera is expressed at levels equivalent to the those required for the Vav1 chimera to reconstitute normal function. This effect cannot be explained by a reduction in TCR expression (Fig. S1).

The SH domains of Vav1 and Vav2 are functionally interchangeable

The ability of Vav1 to support Ca^{2+} responses in T cells has been linked to its participation in SLP-76 microclusters (Sylvain et al., 2011; Ksionda et al., 2012). To determine whether Vav2 disrupts or participates in these structures, Vav isoforms were tagged with mYFP and expressed in a J.Vav1-derived cell line that stably express a red fluorescent SLP-76 chimera (J.Vav1.ST). As reported, mYFP-transfected J.Vav1.ST cells generate unstable SLP-76 microclusters after stimulation on anti-CD3ε-coated glass surfaces (Fig. 1E, bottom row). In contrast, Vav2 enters, stabilizes and promotes the centripetal movement of SLP-76 microclusters to the same level as does Vav1 (Fig. 1E, top and middle rows). Since the subcellular localization of Vav proteins is regulated by a C-terminal adaptor-like region that consists of an SH2 domain flanked by two SH3 domains, we next tested whether these regions in Vav1 and Vav2 are functionally equivalent (Wu et al., 1995; Sylvain et al., 2011; Ksionda et al., 2012). Indeed, a Vav1 chimera in which this C-terminal region was replaced with the corresponding region of Vav2 supports TCR-induced Ca^{2+} responses that are equivalent to those observed with wild-type Vav1 (Fig. 2A). Therefore, any differences in the adaptor functions of these domains are largely irrelevant to the differential impacts of Vav1 and Vav2 on TCR-mediated Ca^{2+} entry.

The CH domain of Vav2 supports TCR-induced Ca^{2+} responses

Despite the antagonistic function of Vav2 in T cells, the CH domains of Vav1 and Vav2 are required for these proteins to enhance antigen receptor-initiated Ca^{2+} responses in T cells and B cells, respectively (Billadeau et al., 2000; Doody et al., 2000; Cao et al., 2002; Zugaza et al., 2002; Sylvain et al., 2011). However, an intra-domain chimera that replaces the N-terminal 20 amino acids of the Vav1 CH domain with the equivalent residues from Vav2 failed to support Ca^{2+} signaling in T cells, raising doubt regarding the functionality of the Vav2 CH domain in T cells (Li et al., 2013). As observed previously, a fluorescently tagged Vav1 chimera lacking the CH domain suppresses the TCR-induced Ca^{2+} responses of J.Vav1 cells to a similar extent to the suppression mediated by wild-type Vav2 (Fig. 2A, Vav1.ΔCH 'High'). The simultaneous inactivation of the Vav1 GEF revealed that this antagonistic effect is not driven by the enhanced GEF activity of this chimera (Fig. 2A, Vav1.ΔCH.LK-AA) (Saveliev et al., 2009). Finally, while the CH domain of a related GEF, αPIX (also known as ARHGEF6), is incapable of restoring the Ca^{2+}-promoting activity of Vav1 (Fig. 2A, Vav1.[CH-αPIX]), the replacement of the entire Vav1

Journal of Cell Science (2020) 133, jcs238337. doi:10.1242/jcs.238337

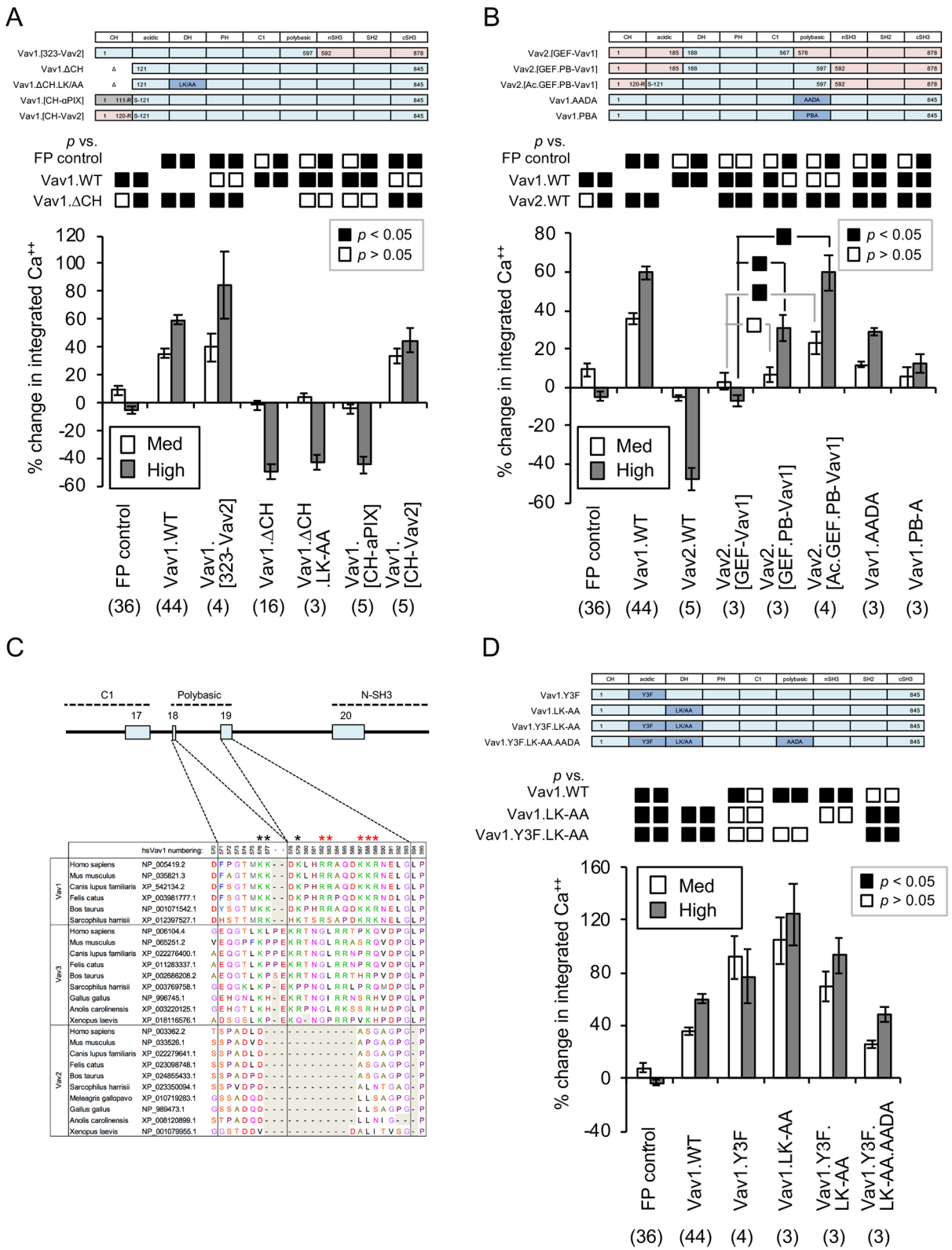

Fig. 2. See next page for legend.

CH domain with the corresponding region of Vav2 reconstitutes this function, at both low and high doses (Fig. 2A, Vav1.[CH-Vav2]). This is consistent with the hypothesis that the CH domains of Vav proteins, but not αPIX, interact with a shared effector of TCR-mediated Ca^{2+} function (Billadeau et al., 2000).

A polybasic linker region C-terminal to the catalytic core of Vav1 is required for TCR-mediated Ca^{2+} entry

By the process of elimination, these findings suggested that the Ca^{2+}-promoting function that is lacking in Vav2 resides within the catalytic 'GEF' core of Vav1, which is an integrated structural unit

Journal of Cell Science (2020) 133, jcs238337. doi:10.1242/jcs.238337

Fig. 2. The differences in the abilities of Vav1 and Vav2 impact Ca^{2+} entry in T cells are encoded by the catalytic core and adjacent linker regions. (A) Truncated and domain swapped variants of Vav1 were constructed as depicted. Domains are color coded by their protein of origin, as in Fig. 1A. C-terminal fluorescent protein tags are not shown. J.Vav1 cells were transiently transfected with constructs encoding the indicated chimeras, loaded with Indo-1 and TCR-induced Ca^{2+} responses were monitored by flow cytometry, as in Fig. 1C. The percent changes in the integrated Ca^{2+} responses of the moderate and high mYFP-expressing populations were calculated relative to non-transfected, mYFP non-expressing cells within the same sample, as in Fig. 1D. Graphs depict the cumulative mean±s.e.m. for all salient experiments. The number of independent replicates is shown in parentheses. Small boxes above each chart depict *P*-values for statistical comparisons between cells expressing matched levels of the chimeras indicated directly below and at left. (B) As in A, with the inclusion of boxes depicting *P* values for statistical comparisons between the Vav2.[GEF-Vav1] chimera and the Vav2.[GEF.PB-Vav1] and Vav2.[Ac.GEF.PB-Vav1] chimeras, when expressed at matched levels. (C) Upper, the genomic structure of the locus encoding the polybasic region of Vav1 is shown. Lower, the sequences of Vav1, Vav2 and Vav3 were manually aligned using known exon boundaries and homology as guides. (D) As in A, for the constructs indicated.

comprising the Dbl homology (DH), a pleckstrin homology (PH) and C1 domains (Booden et al., 2002; Chrencik et al., 2008; Rapley et al., 2008). However, when this region of Vav1 is swapped into Vav2 and the resulting chimera is expressed in J.Vav1 cells, the chimera is inert with respect to Ca^{2+} entry (Fig. 2B, Vav2.[GEF-Vav1]). The further inclusion of a short polybasic (PB) linker immediately C-terminal to the C1 domain of Vav1 enables TCR-induced Ca^{2+} responses that are significant, but weak relative to those of wild-type Vav1 (Fig. 2B, Vav2.[GEF.PB-Vav1]; Fig. 2C). A closer examination of this region of Vav1 revealed that it is extremely well conserved across the tetrapod lineage, where it is encoded in its entirety by two independent exons (Fig. 2C). A distinct, but similarly charged, motif is conserved in Vav3. In contrast, lysine, arginine and histidine residues are absent from this region of Vav2. The transposition of the corresponding region of Vav2 into Vav1 impairs the ability of Vav1 to promote TCR-mediated Ca^{2+} entry (Fig. S2A, Vav1.[PB-Vav2]). Furthermore, the incorporation of the Vav2 PB region into Vav1 chimeras that contain the Src homology module of Vav2 significantly attenuates the Ca^{2+} responses observed with the parental chimera (Fig. S2A, Vav1.[PB323-Vav2] versus Vav1.[323-Vav2]). Next, we generated Vav1–mYFP chimeras with mutations that reduce or eliminate the basic character of this region: the 'AADA' point mutant, which converts three lysine residues into alanine (Fig. 2C, black asterisks), and the 'PB-A' substitution, which replaces all lysine and arginine residues with alanine (Fig. 2C, black and red asterisks). Both mutations significantly reduce the ability of Vav1 to support TCR-initiated elevations in intracellular Ca^{2+} in J.Vav1 cells, with the more-severe 'PB-A' mutation nearly eliminating this response (Fig. 2B). In addition, the AADA and PB-A mutations both impair the upregulation of CD69 in response to TCR ligation (Fig. S2B). However, neither mutation interferes with the TCR-induced tyrosine phosphorylation of Vav1 (Fig. S2C).

The acidic linker region of Vav1 impacts TCR-induced Ca^{2+} entry

Vav2 chimeras that contain the acidic (Ac) regulatory linker from Vav1, as well as the GEF core and polybasic region of Vav1, reconstitute Ca^{2+} responses that approach those of wild-type Vav1 (Vav2.[Ac.GEF.PB-Vav1]). This raised the possibility that the tyrosine residues within this region (Y142, Y160 and Y174) possess Ca^{2+}-promoting scaffolding roles in addition to their roles in the regulation of GEF activity, as has been suggested by the Bustelo group (Barreira et al., 2014, 2018). However, mutations impacting these tyrosine residues also destabilize the conformationally closed, catalytically inert state of Vav1 (Fig. 2D, Vav1.Y3F). The Bustelo group addressed this issue by pre-emptively destabilizing the closed state of Vav1 via the mutation of a distal tyrosine residue. In an analogous manner, we used the catalytically inactivating L334A/K335A mutations to destabilize the closed state and to enhance the Ca^{2+}-promoting function of Vav1 (Fig. 2D, Vav1.LK-AA) (Sylvain et al., 2011). Vav1 chimeras containing the dual Y3F.LK-AA mutations are less effective in promoting Ca^{2+} entry than the LK-AA mutant alone (Fig. 2D, Vav1.Y3F.LK-AA). However, this effect is not significant, and the Ca^{2+} response, although attenuated, remains greater than the wild-type response. In contrast, the mutation of the PB region significantly attenuates the Ca^{2+} responses observed with the Vav1.Y3F.LK-AA mutant (Fig. 2D, Vav1.Y3F.LK-AA.AADA). These findings further highlight the distinctive role of the polybasic region of Vav1 and are consistent with the hypothesis that features within the acidic region of Vav1 contribute to the generation of optimal Ca^{2+} responses.

Vav2 inhibits Ca^{2+} signaling via a catalytic mechanism

As noted above, the antagonistic effect of Vav2 is neutralized by the replacement of its catalytic core with that of Vav1, demonstrating that this region is required for the suppressive function of Vav2 in J.Vav1 cells. The reciprocal experiment reveals that the GEF core of Vav2 is sufficient to convert Vav1 into an antagonist of TCR-mediated Ca^{2+} entry, raising the possibility that the catalytic function of Vav2 contributes to the suppression of TCR-mediated Ca^{2+} signals (Fig. 3A,B). The introduction of the inactivating L337A/K338A (LK-AA) mutation into the catalytic cores of the Vav2 and Vav1.[GEF-Vav2] chimeras reduces the suppressive potencies of these proteins by 60–70%. Given that catalytically inactive Vav1 augments Ca^{2+} entry (Fig. 2D), the inability of the Vav1.[GEF-Vav2.LK-AA] chimera to enhance Ca^{2+} entry demonstrates that the domains comprising the GEF core also contribute to the Ca^{2+}-promoting activity of Vav1 via non-catalytic mechanisms. These findings establish a fundamental asymmetry between the Ca^{2+} influx-promoting activity of Vav1, which is non-catalytic and dependent upon motifs absent in Vav2, and the Ca^{2+} influx-suppressing activity of Vav2, which is significantly dependent on the catalytic activity of the GEF module (Kuhne et al., 2000; Miletic et al., 2009; Saveliev et al., 2009; Sylvain et al., 2011).

Activated Rho family GTPases have divergent impacts on Ca^{2+} signaling in T cells

Based on these findings, we reasoned that a unique substrate of Vav2 could be responsible for the inhibition of TCR-initiated Ca^{2+} signals by Vav2. To test this hypothesis, we generated TagRFP-Turbo (TRT)-tagged constitutively active (CA) forms of Rho family GTPases reported as substrates of the Vav family members and expressed these chimeras in J.Vav1 cells (Fig. 3C). The active form of Rac1, which is a well-documented target of both Vav1 and Vav2, increases TCR-induced Ca^{2+} responses when expressed at high levels (Fig. 3D). The active form of Rac2 enhances Ca^{2+} responses in a similar manner, but is also effective when expressed at moderate levels. The behavior of the CA form of RhoG is similar to Rac1, while the CA form of RhoA is neutral with respect to TCR-mediated Ca^{2+} elevations. In contrast, the CA form of Cdc42 potently inhibits TCR-dependent Ca^{2+} responses in J.Vav1 cells. The impact of Cdc42 does not require a specific activating mutation, as the G12V and Q61L mutants yield similar results (Fig. S3A). In addition, the

Journal of Cell Science (2020) 133, jcs238337. doi:10.1242/jcs.238337

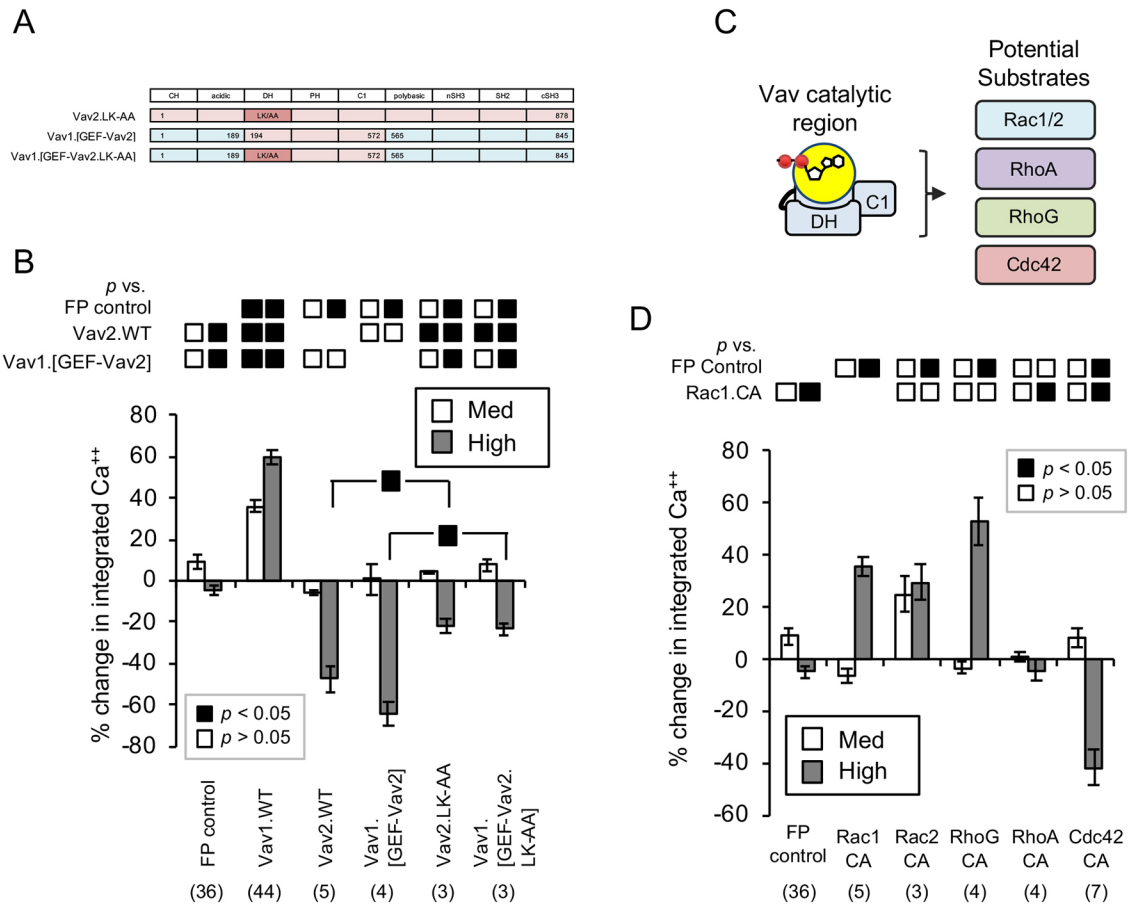

Fig. 3. Vav2 affects Ca^{2+} influx by a catalytic mechanism. (A) Vav chimeras used in B. Pertinent domain swaps and the GEF-inactivating L337A/K338A (LK-AA) mutation are depicted. The LK-AA mutation is analogous to the mutation used in Vav1; the region surrounding these amino acids is invariant between Vav1 and Vav2. (B) The indicated chimeras were transfected into J.Vav1 cells and Ca^{2+} responses were measured, quantified and statistically analyzed as in Fig. 2. (C) Rho family GTPases reported to be activated by Vav family GEFs. (D) The impacts of constitutively active (CA) forms of the indicated Rho GTPases on TCR-initiated Ca^{2+} elevations were analyzed as in Fig. 2. Ca^{2+} responses were simultaneously assessed for cells expressing the indicated levels of the 3×Flag.TRT-tagged GTPases. The calculations presented are for pooled Cdc42 data obtained with both splice isoforms of Cdc42 and with distinct activating mutations (see Fig. S3).

atypically lipidated Cdc42 splice isoform found in brain tissue suppresses TCR-initiated Ca^{2+} responses as well as the common, prenylated splice isoform present in hematopoietic cells (Fig. S3A,B) (Olenik et al., 1999; Nishimura and Linder, 2013; Wirth et al., 2013). To evaluate whether endogenous Rac1 and Cdc42 regulate Ca^{2+} responses, we transiently knocked down these GTPases (Fig. S4A). The suppression of Rac1 has a marginal impact on TCR-induced Ca^{2+} responses in J.Vav1 cells reconstituted with wild-type Vav1 (Fig. S4B, green line slightly below red line). Nevertheless, the global inhibition of all Rac isoforms using EHT-1864 profoundly impairs the TCR-induced Ca^{2+} responses of wild-type Jurkat E6.1 cells (Fig. S4C) (Shutes et al., 2007). These data are consistent with the role of Rac2 in antigen receptor-dependent Ca^{2+} responses (Yu et al., 2001; Croker et al., 2002; Baier et al., 2014). In contrast, the suppression of Cdc42 enhances the Ca^{2+} responses of J.Vav1 cells (Fig. S4D, green line displaced above red line), suggesting that the activation of endogenous Cdc42 antagonizes TCR-mediated Ca^{2+} entry in these cells (Phee et al., 2005).

The interactions of full-length Vav GEFs and Rho GTPases can be imaged in intact cells

The simplest interpretation of these findings is that Vav2, but not Vav1, directly activates Cdc42, which in turn inhibits TCR-induced Ca^{2+} elevations. However, the literature regarding the activity of Vav2 towards Cdc42 is contradictory, with some *in vitro* kinetic studies identifying Vav2 as a potent Cdc42 GEF, and others finding that Vav2 has virtually no activity towards Cdc42 (see Discussion) (Abe et al., 2000; Booden et al., 2002; Heo et al., 2005; Jaiswal et al., 2013). In contrast, there is no controversy regarding the abilities of Vav1, Vav2 and Vav3 to activate Rac1, or the inability of Vav1 and Vav3 to activate Cdc42 (Chrencik et al., 2008; Rapley et al., 2008; Barreira et al., 2014). Therefore, we developed an imaging assay capable of visualizing the interactions between Vav GEFs and Rho GTPases in the more-physiological context of intact T cells. GEF–GTPase interactions are difficult to visualize because the interaction of a GTPase with its GEF is rapidly terminated following the GEF-induced acquisition of GTP by the GTPase (Fig. 4A). However, dominant-negative (DN) forms of the Rho GTPases have a low affinity for GTP and can remain locked in the nucleotide-free GEF-bound state (Fig. 4A) (Feig, 1999). Since both Vav1 and Vav2 clearly enter SLP-76 microclusters (Fig. 1E), we reasoned that it would be possible to visualize the co-accumulation of DN Rho GTPases with physiologically activated Vav isoforms in SLP-76 microclusters.

To test the viability of this ‘GEF trap’ strategy, we employed a TRT-tagged DN (T17N) form of Rac1. This GTPase was co-

Journal of Cell Science (2020) 133, jcs238337. doi:10.1242/jcs.238337

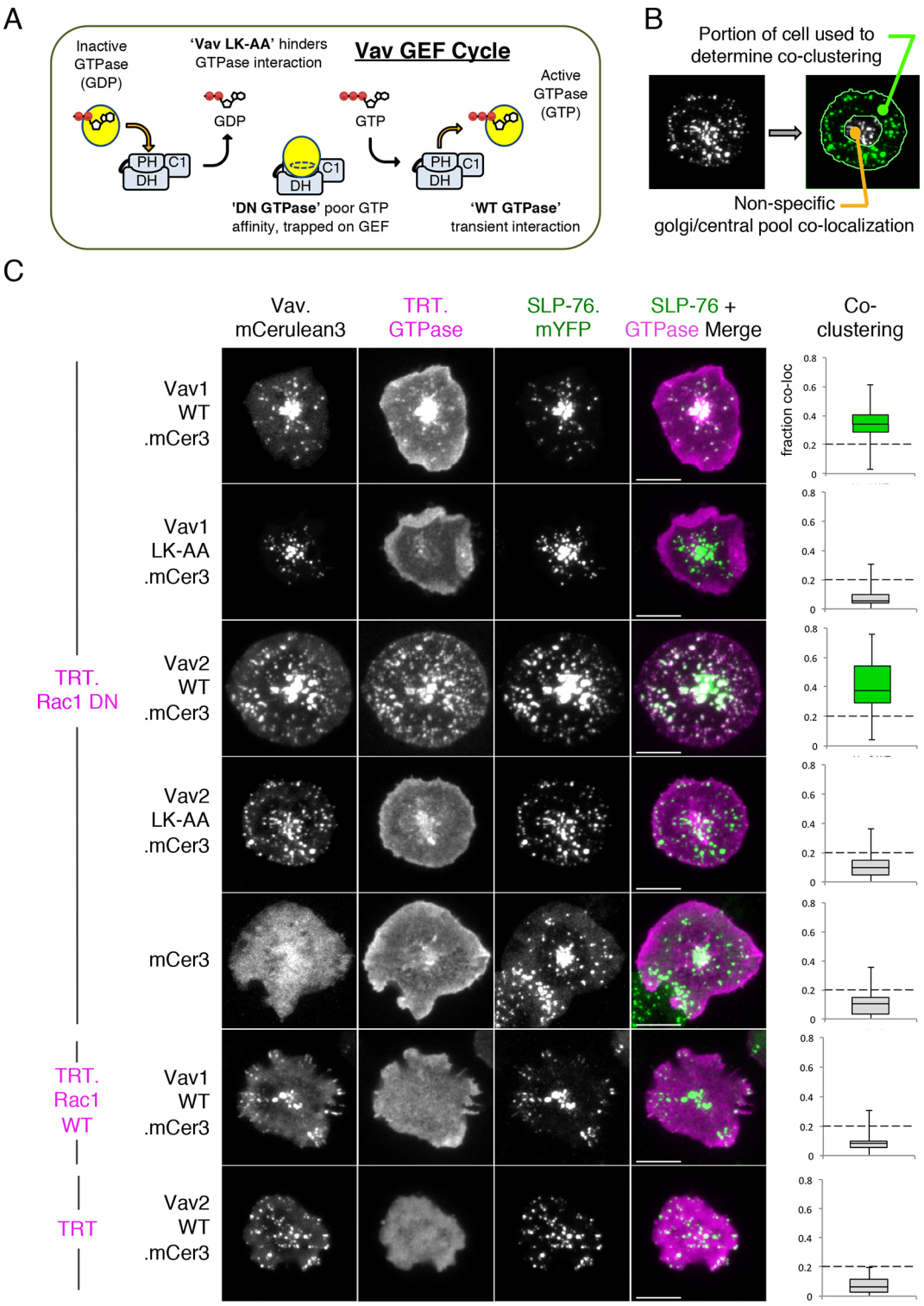

Fig. 4. The interaction of Rac1 with the catalytic surfaces of Vav1 and Vav2 can be visualized in intact cells. (A) Schematic of the 'GEF trapping' imaging strategy. GEF–GTPase interactions are difficult to image as they are rapidly destabilized upon the acquisition of GTP by the GTPase. The dominant-negative (DN) GTPase mutants used here remain bound to the catalytic surface of the GEF due to low GTP affinity. The Vav GEF-inactivating LK-AA mutation disrupts the GEF–GTPase interface. (B) The outermost 80% of the stimulatory interface is highlighted in green to emphasize the region considered when determining co-clustering. (C) Visualization of TRT-tagged Rac1 chimeras (magenta pseudocolor) and mCer3-tagged Vav chimeras in cells that stably express a YFP-tagged SLP-76 chimera (J14.SY cells) (green pseudocolor). Cells were plated on OKT3-coated glass surfaces and fixed after 7 min. Cells at peak spreading were selected for analysis. Each row of images corresponds to one representative cell. For clarity, the Vav channel is omitted from the merge image, as all Vav constructs colocalize with SLP-76. Scale bars: 10 µm. The co-clustering column shows an average of the fractional overlaps of the clustered areas identified using the GTPase and SLP-76 channels (see Materials and Methods). Boxes enclose the second and third quartiles and whiskers indicate minimum and maximum values. Interquartile boxes are colored green if the colocalization score is statistically indistinguishable from or greater than that observed for the Vav1.WT and Rac1.DN pair. Amounts below the dashed line correspond to no visible co-clustering. Statistical data and replicate numbers are provided in Fig. S4A.

Journal of Cell Science (2020) 133, jcs238337. doi:10.1242/jcs.238337

expressed at moderate levels with mCerulean3 (mCer3)-tagged Vav GEFs in SLP-76-deficient Jurkat cells that had been stably reconstituted with SLP-76–mYFP (J14.SY cells) (Bunnell et al., 2002). These cells were then stimulated on stimulatory coverslips in order to elicit T cell activation and the formation SLP-76 microclusters. Because SLP-76 microclusters accumulate in the center of the contact near a perinuclear pool of Rho GTPases, we excluded a central region corresponding to 20% of the area of the contact from our colocalization analyses to minimize spurious colocalization signals (Fig. 4B) (Erickson et al., 1996). Wild-type Rac1 does not colocalize with SLP-76 microclusters (Fig. 4C; Fig. S5A). In contrast, DN Rac1 colocalizes with microclusters containing either wild-type Vav1 or Vav2 (Fig. 4C; Fig. S5A). The interaction of DN Rac1 with Vav1 or Vav2 involves the catalytic surface on these GEFs, as DN Rac1 fails to colocalize with the GEF-dead Vav1.LK-AA and Vav2.LK-AA mutants, which alter the central Rac1-binding surface of the DH domain (Fig. 4C; Fig. S5A) (Saveliev et al., 2009). Finally, the recruitment of DN Rac1 to microclusters requires the concurrent overexpression of a Vav isoform, as it is not apparent when a mCer3 control is used in lieu of the Vav chimeras (Fig. 4C, mCer3 with TRT.Rac1.DN; Fig. S5A). This confirms that the recruitment of Rac1 into microclusters is controlled by the overexpressed Vav1 and Vav2 chimeras, and is not caused by DN Rac1 overexpression. These observations are consistent with the involvement of both Vav1 and Vav2 in TCR-induced nucleotide exchange on Rac1.

Vav1 and Vav2 show different GTPase specificities *in vivo*

Having established the viability of the 'GEF trap' assay with Rac1, we assessed other GTPases. Remarkably, no GTPase other than Rac1 displayed clear colocalization with Vav1, while Vav2 'trapped' a broader range of Rho GTPases (Fig. 5A,B; Fig. S5B). A fraction of Rac2 colocalizes with Vav2, forming faint clusters that are coincident with SLP-76 (Fig. 5A, top row; Fig. S5B). Although RhoA is often reported as a target of Vav1 and Vav2 (Booden et al., 2002; Barreira et al., 2014), DN RhoA is not visibly recruited into Vav1- or Vav2-containing SLP-76 microclusters (Fig. 5A, second row; Fig. S5B). RhoG is also activated following TCR ligation, and a functional interaction between Vav2 and RhoG has been reported (Schuebel et al., 1998; Martínez-Martín et al., 2011). However, cells expressing DN RhoG fail to spread on substrates coated with anti-CD3ε alone. To facilitate T cell attachment without altering SLP-76 microcluster induction and movement, these cells were plated on substrates bearing anti-CD3ε and anti-CD43 (Bunnell et al., 2002; Nguyen et al., 2008). Under these conditions, DN RhoG partially overlapped with Vav2-containing, but not Vav1-containing, microclusters (Fig. 5A, third row; Fig. S5B). The most remarkable difference between Vav1 and Vav2 is the ability of Vav2, but not Vav1, to capture DN Cdc42 within SLP-76 microclusters (Fig. 5B; Fig. S5B). The GEF core of Vav2, which conveys inhibition of TCR-induced Ca^{2+} responses into Vav1, also conveys the ability to trap Cdc42 into Vav1 chimeras (Fig. 5B, Vav1.WT versus Vav1.[GEF-Vav2]; Fig. S5B). Furthermore, the Vav2.LK-AA catalytic surface mutant is incapable of trapping DN Cdc42 (Fig. 5B, Vav2.LK-AA; Fig. S5B). These observations are consistent with the hypothesis that Vav2 inhibits TCR-mediated Ca^{2+} responses via the activation of Cdc42.

The DH domains of Vav1 and Vav2 distinguish Cdc42 from Rac1 via Cdc42^{F56}

The experiments above establish that the DH-PH-C1 modules of Vav1 and Vav2 determine their specificity for Cdc42. Although the canonical GTPase-binding site lies within the DH domain, we postulated that the interconnected PH and C1 domains might influence the binding specificity of the overall GEF core. To test this hypothesis, we swapped individual domains of Vav1 into Vav2 and screened for the loss of DN Cdc42 binding (Fig. 6A). This approach allowed us to use the retention of DN Rac1 binding as a positive control for the folding of the chimeric GEF core. All three hybrid proteins bind DN Rac1 (Fig. 6B, right column; Fig. S5C), indicating that these chimeras are properly folded. The C1 and PH domains of Vav1 do not impair the interaction of Vav2 with Cdc42, indicating that these domains are not responsible for the exclusion of Cdc42 from Vav1 (Fig. 6B, left column; Fig. S5C). In contrast, the Vav1 DH domain impairs the interaction of Vav2 with Cdc42, confirming that this domain is the primary determinant of Vav GEF specificity (Fig. 6B, left column). To further investigate the mechanism by which Cdc42 is excluded from Vav1, we generated DN chimeric GTPases from Cdc42 and Rac1 (Fig. 6C). The resulting chimeras were screened for colocalization with Vav1 and Vav2. All chimeras colocalize with Vav2 in SLP-76 microclusters, indicating that they are properly folded (Fig. 6D, right column). The first round of screening revealed that the N-terminal region determines the selective binding of the chimeric GTPase to Vav1 (Fig. 6D, rows 1–2; Fig. S5D). In contrast, the effect of constitutively active versions of these hybrid GTPases on TCR-induced Ca^{2+} entry is determined by the C-terminal portion of the GTPase (Fig. S6A). A second round of screening showed that amino acids 1 through 45 of Rac1 have a marginal positive impact on the binding of Cdc42 to Vav1 (Fig. 6D, row 3; Fig. S5D). In contrast, a fragment of Rac1 (amino acids 46–76) containing the β3 strand, the switch II region and the α2 helix clearly enables Cdc42 to 'trap' with Vav1 (Fig. 6D, row 4; Fig. S5D). Within this region, only six amino acids differ between Rac1 and Cdc42 (Fig. S6B). When divergent residues from this segment of Rac1 are introduced into Cdc42 in groups of one or two amino acids, only the Cdc42 F56W mutant colocalizes with Vav1 and Vav2 (Fig. 6D, Cdc42 F56W, row 5; Fig. S5D; Fig. S6C). All other point mutations affecting this region of Cdc42 colocalize with Vav2 but not with Vav1 (Fig. S6C). These observations indicate that the presence of a phenylalanine residue at position 56 precludes the interaction of Cdc42 with the DH domain of Vav1 in SLP-76 microclusters.

Vav2 inhibits Ca^{2+} influx in Jurkat cells by activating Cdc42

Since Vav2 is capable of interacting with Cdc42 and since Cdc42 suppresses TCR-initiated Ca^{2+} responses, we wished to determine whether the inhibitory potential of Vav2 is mediated by Cdc42. To do so, we took advantage of ZCL28, a small-molecule inhibitor of Cdc42 that does not interfere with Rac1 or RhoA function (Friesland et al., 2013). Crucially, ZCL278 was specifically designed to block the activation of Cdc42 by GEFs by occupying a selectivity pocket that incorporates F56 of Cdc42, which is unique within the Rho GTPase family. The addition of this inhibitor to Indo-1-labeled J.Vav1 cells leads to a gradual rise in basal Ca^{2+} levels, increasing the algorithmically determined baseline that is subtracted from the integrated Ca^{2+} response (Fig. 7A, basal). Nevertheless, ZCL278 permits the measurement of acute changes in cytoplasmic Ca^{2+} levels following TCR stimulation. We first compared the impacts of ZCL278 on wild-type and LK-AA mutant Vav2 chimeras because Vav2 retains a portion of its suppressive potency when it is catalytically inactive (Fig. 3A,B). Whereas ZCL278 does not significantly alter the Ca^{2+} responses of TCR-stimulated J.Vav1T cells expressing a catalytically inert

Journal of Cell Science (2020) 133, jcs238337. doi:10.1242/jcs.238337

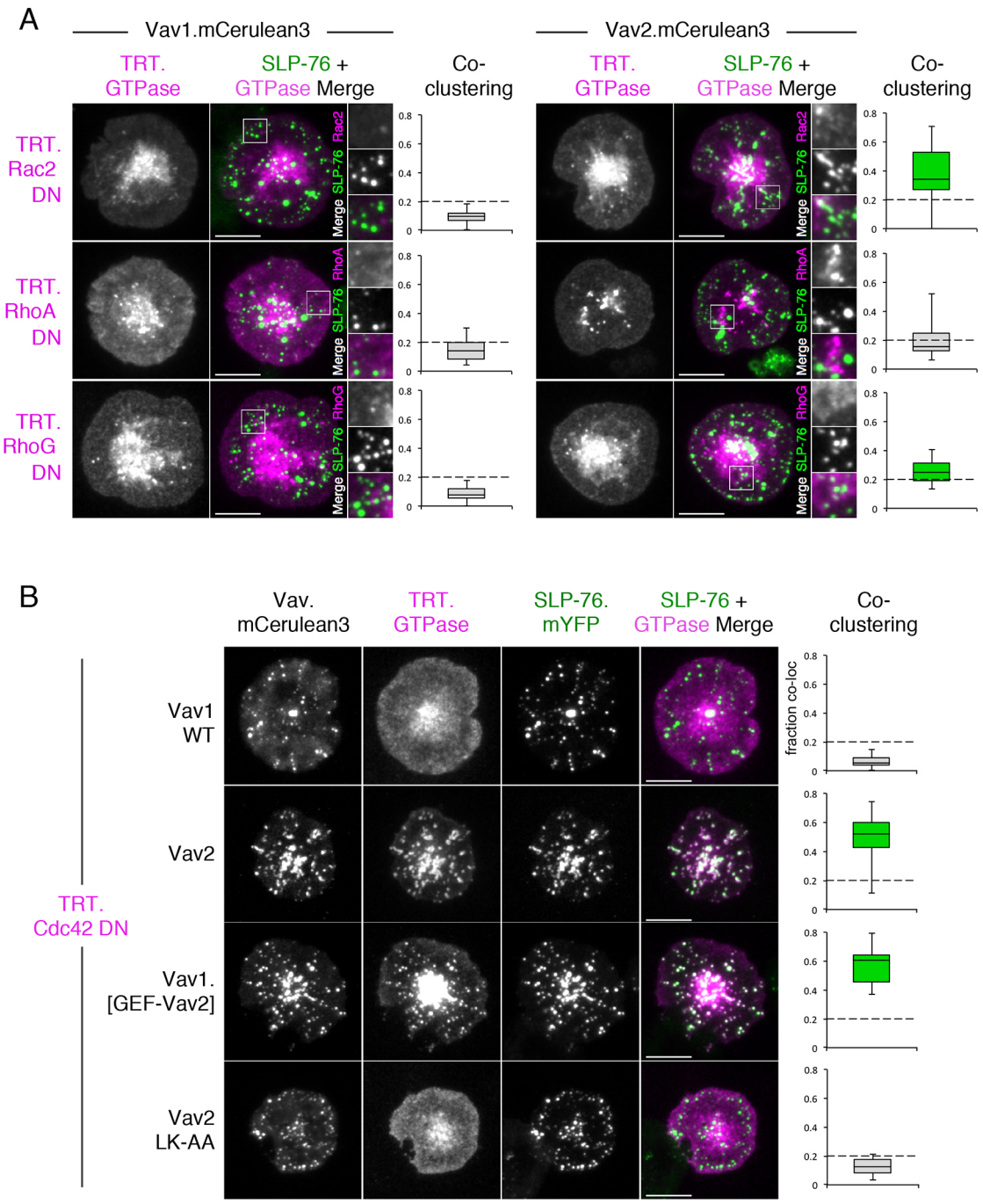

Fig. 5. Vav2 traps a broader range of Rho GTPases than Vav1. (A) J14.SY cells were co-transfected with vectors encoding a TRT-tagged DN chimera of Rac2, RhoA or RhoG, and mCer3-tagged chimeras of either wild-type Vav1 (left panels) or Vav2 (right panels). Cells were imaged as in Fig. 4B, with the exception of DN RhoG, which required co-coating the plate with anti-CD3 and anti-CD43 to assist with cell retention. The left column of each group is a grayscale image of the GTPase channel. The pseudocolored image depicts the DN GTPase (magenta) and SLP-76 (green). Both Vav isoforms colocalize with SLP-76 and have been omitted for clarity. Boxed regions are magnified 2× at right; individual grayscale images of the GTPase and SLP-76 are shown for clarity. Co-clustering was quantified as in Fig. 3. (B) J14.SY cells were co-transfected with vectors encoding a TRT-tagged DN Cdc42 chimera and the indicated mCer3-tagged Vav chimeras and mutants. Images were acquired and presented as in Fig. 3B. Statistical data and replicate numbers are provided in Fig. S4B. Scale bars: 10 µm.

Vav2.LK-AA control, ZCL278 robustly inhibits the suppression of TCR-initiated Ca^{2+} responses by wild-type Vav2 (Fig. 7A, upper and middle rows; Fig. 7B). To control for potential off-target 'anti-inhibitory' effects of ZCL278, we also examined the ability of this compound to attenuate the suppressive effects of constitutively activated Cdc42. Since ZCL278 targets the interaction of Cdc42 with its GEFs, the suppressive effects of CA Cdc42 should resist inhibition by ZCL278, as CA Cdc42 interacts with its downstream effectors in a GEF-independent manner. Indeed, ZCL278 does not significantly attenuate the suppressive effect of CA Cdc42 on TCR-initiated Ca^{2+} responses (Fig. 7A, lower row; Fig. 7B). Finally, we confirmed that the ability of Vav2 to suppress TCR-induced Ca^{2+} responses is virtually eliminated following the shRNA-mediated suppression of endogenous Cdc42 (Fig. S4A;

Journal of Cell Science

Journal of Cell Science (2020) 133, jcs238337. doi:10.1242/jcs.238337

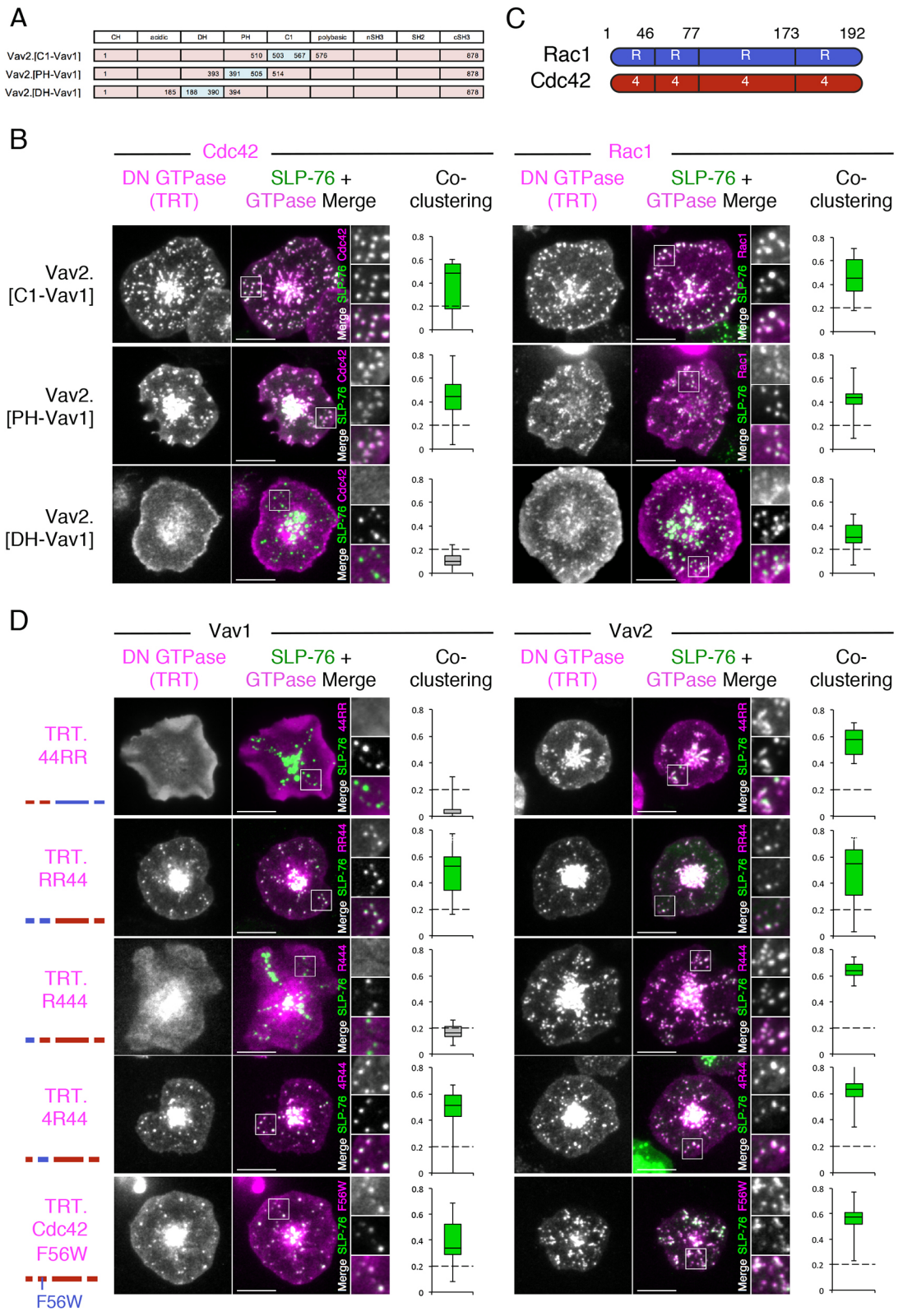

Fig. 6. The refinement of the surfaces that mediate the selective interaction between Vav2 and Cdc42. (A) Schematic of the domain-swapped Vav constructs used in B. Individual domains within Vav2 (red) were replaced by the corresponding domains from Vav1 (blue). (B) J14.SY cells were co-transfected with vectors encoding a TRT-tagged dominant-negative (DN) Rac1 or Cdc42 chimera and the indicated mCer3-tagged Vav chimeras. Images and quantifications were acquired and presented as in Fig. 5. Statistical data and replicate numbers are provided in Fig. S4C. (C) Schematic depicting the breakpoints for the Rac1 and Cdc42 chimeras used below. Blue or 'R' represents Rac1, and red or '4' represents Cdc42. (D) J14.SY cells were co-transfected with vectors encoding a TRT-tagged DN Rac1–Cdc42 chimera and either mCer3-tagged Vav1 (left) or Vav2 (right). Bars at the far left identify the GTPase of origin for each segment of the chimera (Rac1, blue; Cdc42, red). Images and quantifications were acquired and presented as in Fig. 5. Statistical data and replicate numbers are provided in Fig. S4D.

Journal of Cell Science (2020) 133, jcs238337. doi:10.1242/jcs.238337

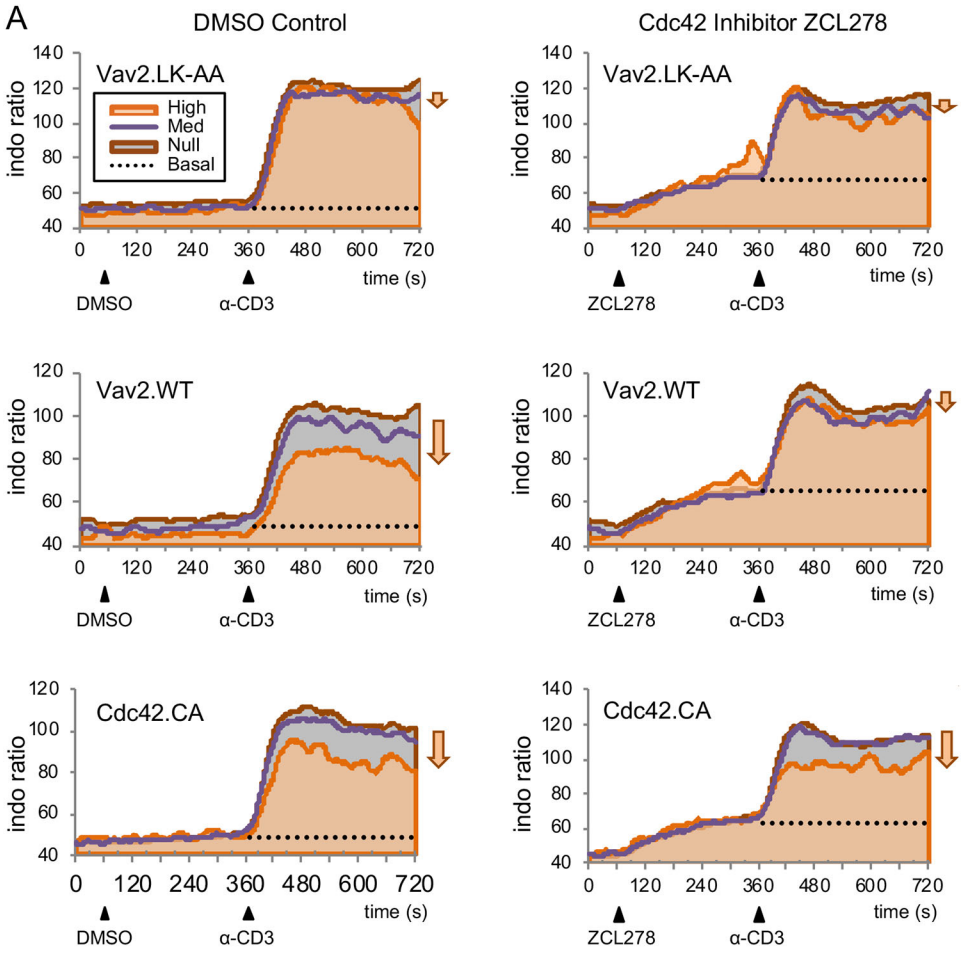

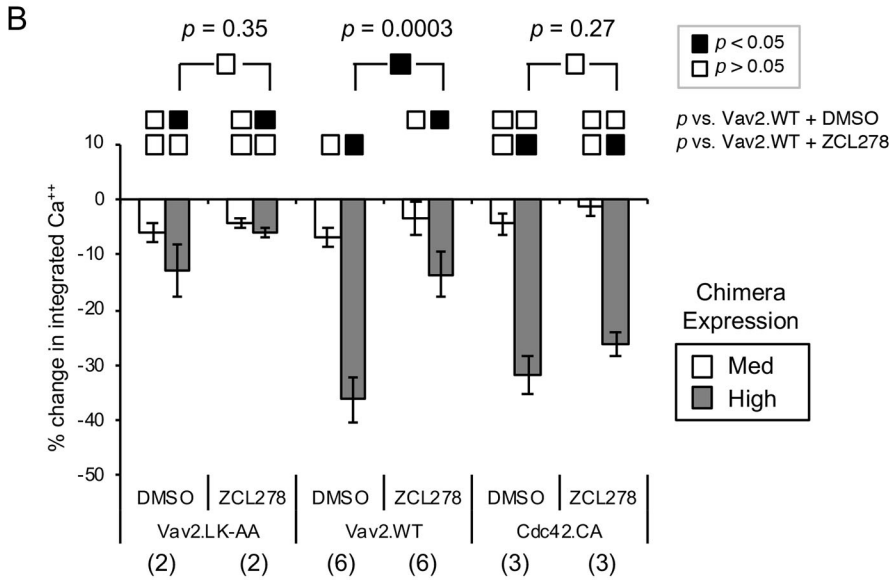

Fig. 7. Vav2 acts through Cdc42 to inhibit TCR-induced Ca^{2+} responses. (A) Representative Ca^{2+} response graphs comparing the effects of ZCL278, an inhibitor of Cdc42 activation, on the suppression of Ca^{2+} influx by Vav2 and constitutively active (CA) Cdc42. Baseline reads were collected for 60 s, after which either ZCL278 (100 µM final) or an equivalent amount of DMSO was added. After 5 min, OKT3 (α-CD3) was added and readings were collected for an additional 6 min. Arrows on the right emphasize the shift in Ca^{2+} entry observed between non-expressing and highly expressing cells in the same tube. (B) Ca^{2+} responses were quantified as in Fig. 1. Graphs depict the mean±s.e.m. percentage change in the integrated Ca^{2+} responses of the moderate and high mYFP-expressing cells relative to non-expressing cells within the same sample ($n \geq 3$ for all conditions).

Fig. S7A,B). These observations confirm that heterologously expressed Vav2 inhibits TCR-stimulated Ca^{2+} responses via its action on Cdc42.

DISCUSSION

These studies have exploited the heterologous expression of Vav2, and of various Vav mutants and chimeras, as a tool to clarify which aspects of Vav function that are shared between Vav1 and Vav2, and which are distinctive. These studies revealed that the CH domain and the C-terminal adaptor-like region of Vav2 support TCR-initiated Ca^{2+} elevations as elements of Vav1 chimeras. These studies also defined fundamental asymmetries in the functions of Vav1 and Vav2. Specifically, Vav1 facilitates Ca^{2+} signaling downstream of the TCR via non-catalytic

Journal of Cell Science (2020) 133, jcs238337. doi:10.1242/jcs.238337

mechanisms that involve a highly conserved polybasic motif that is absent from Vav2. In contrast, the ability of Vav2 to antagonize the same Ca^{2+} signals depends on its catalytic activity and is mediated by Cdc42, which is not efficiently targeted by Vav1 (Fig. 8).

Biochemical studies have shown that Vav1, Vav2 and Vav3 all interact with phosphorylated forms of SLP-76 via their SH2 domains (Tartare-Deckert et al., 2001; Zakaria et al., 2004; Charvet et al., 2005). Thus, it is not entirely surprising that the SH2 domain-containing portions of Vav1 and Vav2 both support the recruitment of Vav chimeras into SLP-76 microclusters. However, the flanking SH3 domains interact with dozens of proteins that could contribute to differences in isoform function (Bustelo, 2012, 2014). In addition, the linker that joins the SH2 and C-SH3 domains in the long isoform of Vav2 contains an alternatively spliced exon that is absent from Vav1. Nevertheless, our findings indicate that none of these differences influences Ca^{2+} signaling in T cells.

The mechanisms by which the CH domains of Vav isoforms influence antigen-induced Ca^{2+} is somewhat controversial. All reports agree that the CH domain of Vav1 plays an essential role in the induction of Ca^{2+} responses by the TCR (Billadeau et al., 2000; Cao et al., 2002; Sylvain et al., 2011). The Cao laboratory has attributed this effect to an interaction with calmodulin that is unique to Vav1 (Zhou et al., 2007; Li et al., 2013). However, we find that the CH domain of Vav2 is fully competent to support TCR-induced Ca^{2+} responses in the context of a Vav1 chimera. Furthermore, we

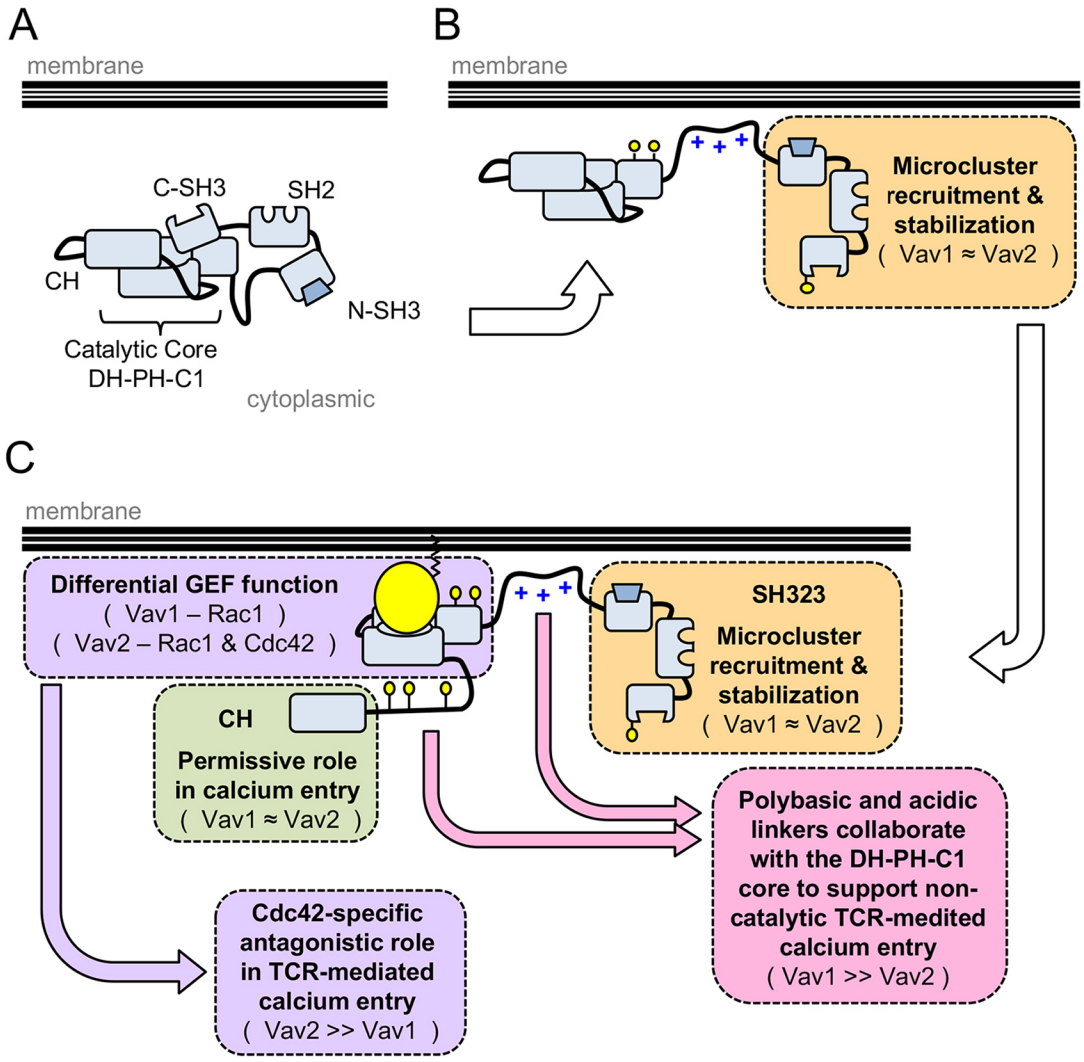

Fig. 8. A model of Vav1 and Vav2 activation and the differential impacts of these GEFs on TCR-induced Ca^{2+} responses. (A) In the resting state, Vav proteins adopt a closed configuration in which N-terminal regulatory linker and the calponin homology (CH) domain occlude the catalytic surface of the DH domain, and interactions between the catalytic core and the C-terminal SH3 domain stabilize this inert configuration. (B) In response to TCR ligation, the C-terminal Src homology domains (orange box) mediate the recruitment of Vav proteins into membrane-associated and tyrosine-phosphorylated signaling complexes, i.e. microclusters. Microcluster-resident kinases then tyrosine phosphorylate (small yellow circles) Vav proteins to initiate their opening. (C) In response to the tyrosine phosphorylation of the regulatory tyrosine residues in their acidic linker regions, the catalytic surfaces of the Vav GEFs are revealed and interact with Rho family GTPases (large yellow circle). With respect to Ca^{2+} signaling, the C-terminal Src homology domains and the N-terminal CH domains are functionally interchangeable between Vav1 and Vav2. The CH domain supports Ca^{2+} entry via as yet uncharacterized mechanisms (green box). Vav1 contains a distinctive and highly conserved polybasic region (blue plus signs) that is absent from Vav2. This region, in conjunction with the acidic linker region, enables Vav1-dependent increases in TCR-mediated Ca^{2+} entry (pink box). Conversely, the ability of Vav2 to interact with Cdc42 is unique among the Vav proteins and contributes to the suppression of TCR-induced calcium responses (purple boxes). Nevertheless, the catalytic activity of Vav2 plays a positive role in BCR-induced Ca^{2+} entry, emphasizing that Cdc42 plays distinct roles in the transmission of antigen-dependent signals in T and B cells.

Journal of Cell Science (2020) 133, jcs238337. doi:10.1242/jcs.238337

note that the CH domain of Vav2 plays a critical role in the enhancement of antigen-receptor-induced Ca^{2+} responses in B cells (Doody et al., 2000). The CH domain of Vav3 may also be permissive of Ca^{2+} entry, as full-length exogenous Vav3 augments the TCR-induced Ca^{2+} responses of J.Vav1 cells (Fig. 1D). In contrast, the CH domain of αPIX is unable to support these responses (Fig. 2A). The simplest interpretation of these findings is that the CH domains of the Vav proteins, but not of αPIX, interact with a common effector of Ca^{2+} signals, arguing against the involvement of calmodulin, which only binds to the CH domain of Vav1, as the decisive factor. The salient factor is of great interest and would be expected to enhance the stability of SLP-76 microclusters, increase the proximity of Vav1 to PLCγ1 and promote the production of inositol 1,4,5-trisphosphate by PLCγ1 (Sylvain et al., 2011; Knyazhitsky et al., 2012).

In contrast to the CH domain, the non-catalytic role of the DH-PH-C1 module of Vav1 in TCR-mediated Ca^{2+} elevations is not conserved in Vav2. This conclusion stems from the observation that the LK-AA mutation in Vav1 enhances Ca^{2+} signals downstream of the TCR, most likely by destabilizing the closed state of the protein, while the analogous mutation has no such effect on a Vav1 chimera that contains the DH-PH-C1 module of Vav2 (Fig. 3B). The salient interactions are not well understood, but, based on prior reports, could involve interactions with phosphoinositides, Rap-family GTPases or the p67 subunit of the phagocyte oxidase complex (Arthur et al., 2004; Prisco et al., 2005; Ming et al., 2007).

Our structure–function analyses also led us to identify an intensely charged polybasic motif as a decisive factor that contributes to the ability of the Vav1 DH-PH-C1 module to support TCR-initiated Ca^{2+} responses via non-catalytic mechanisms (Fig. 2B). The motif lies immediately C-terminal to the C1 domain and is encoded by two small exons. The same two exons encode a similar motif in Vav3, which can also augment Ca^{2+} responses in J.Vav1 cells. Both motifs are rigorously conserved in the tetrapod lineage. The local charge density in these motifs is very high, with six or eight lysine and arginine residues among 14 or 15 contiguous residues. In contrast, this region of Vav2 contains no positively charged residues. Since similar motifs drive electrostatic interactions with phosphoinositide-bearing membranes across a wide range of proteins, we anticipated that this motif would contribute to the recruitment of Vav1 to the plasma membrane, and could, in this manner, influence the orientation of the catalytic core relative to its substrates and binding partners (Heo et al., 2006). Indeed, while this study was in review, the Bustelo group identified the polybasic region as a crucial regulator of Vav1 signaling in T cells and showed that this region collaborates with the neighboring C1 domain to bind inositol monophosphates (Rodriguez-Fdez et al., 2019). Thus, the inability of the Vav2 catalytic core to support normal Ca^{2+} signals in the context of Vav1 may reflect a defect in C1-dependent phosphoinositide recognition.

Among the GTPase substrates tested, our 'GEF trap' assays indicate that full-length Vav1 only binds Rac1, while Vav2 interacts a much broad range of substrates, including Rac1, Rac2, Cdc42 and, to a lesser degree, RhoG. This assay is based on the stable interactions of dominant-negative, GTP non-binding forms of Rho GTPases with their GEFs (Guilluy et al., 2011). The recruitment of Vav GEFs into readily identifiable microclusters enabled us to monitor their interactions with dominant-negative forms of the Rho GTPases *in vivo*, in real time. While these assays cannot provide data regarding rates of nucleotide exchange, they possess unique advantages insofar as they employ full-length proteins post-translationally modified in mammalian cells. This is crucial, as some GEFs only interact with appropriately prenylated GTPases (Hamann et al., 2007). Furthermore, the 'GEF trap' assay is performed in a subcellular context that preserves the interactions of the Rho GTPases and Vav GEFs with intact membranes and their associated signaling complexes, which are likely to impose constraints that are not replicated in standard *in vitro* assays.

In vitro kinetic assessments of the catalytic activities of Vav proteins leave no doubt that Vav1, Vav2 and Vav3 are efficient activators of Rac1, or that Vav1 and Vav3 are poor activators of Cdc42 (Aghazadeh et al., 2000; Chrencik et al., 2008; Rapley et al., 2008; Barreira et al., 2014). Unfortunately, the literature regarding the activity of Vav2 towards Cdc42 has been confounding, with two studies identifying Vav2 as a potent Cdc42 GEF (Abe et al., 2000; Booden et al., 2002), and two studies finding that Vav2 has virtually no activity towards Cdc42 (Heo et al., 2005; Jaiswal et al., 2013). In light of our findings, we reexamined these manuscripts carefully and determined that all four used the same long isoform of human Vav2 used here and that the two studies that found activity towards Cdc42 had employed catalytic fragments that clearly encompass the relevant domains (residues 191–573 or 192–573 versus predicted domain boundaries at residues 202–571; Fig. 1A) (Abe et al., 2000; Booden et al., 2002). We were unable to determine the domain boundaries employed by Heo et al. (2005). The most recent study, which found minimal activity towards Cdc42, appears to have used a catalytic fragment that includes an auto-inhibitory tyrosine at Y172 and that truncates the C1 domain, i.e. 'Vav2 (aa 168-543)' (Jaiswal et al., 2013). Furthermore, the studies that found little activity towards Cdc42 used outlying molar ratios of GEF and GTPase in their kinetic assays [i.e. ∼1:5000 (Heo et al.) and 100:1 (Jaiswal et al.)] versus values ranging from 1:43 to 8:1 for a limited survey of the literature (Leonard et al., 1994; Abe et al., 2000; Booden et al., 2002; Mitin et al., 2007; Chrencik et al., 2008; Rapley et al., 2008; Barreira et al., 2014). Finally, we note that recent studies using a split luciferase reporter or an *in vivo* single-chain FRET biosensor found the activity of Vav2 towards Cdc42 comparable to the activities of Dbl, Dbs and Intersectin2, which are all recognized as effective Cdc42 GEFs (Anderson and Hamann, 2012; Hanna et al., 2014). On balance, these studies are consistent with our *in vivo* 'GEF trap' assays, and suggest that the C1 domain may play an important role in determining the substrate specificity of Vav2.

Our findings suggest the existence of an important dichotomy within the Vav family, separating Vav1 and Vav3 from Vav2. With respect to the two crucial differences identified here, Vav3 possess an alternative polybasic motif and does not interact with Cdc42 (Movilla et al., 2001). The polybasic motifs present in Vav1 and Vav3 are highly conserved within tetrapods, and can also be observed in bony fish. In contrast, these motifs are absent from Vav2 and the Vav paralogs present in earlier branching lineages. Thus, it is likely that their associated signaling functions first emerged during the two rounds of genome duplication that accompanied the establishment of the modern vertebrate lineage (Flajnik and Kasahara, 2010). Similarly, the conserved sequence elements that distinguish the catalytic cores of the Vav GEFs from one another also emerged at this juncture in evolution. Therefore, the scaffolding and catalytic properties that distinguish Vav1 and Vav3 from Vav2 may have played an important role in the establishment of the modern adaptive immune system, which also emerged at this time.

Although we do not yet understand how the differences in the ability to bind Cdc42 are encoded within the DH domains of Vav proteins, we were able to identify a single amino acid that plays a decisive role in ligand discrimination by Vav1. Specifically, a F56W substitution was sufficient to convert Cdc42 into a

Journal of Cell Science (2020) 133, jcs238337. doi:10.1242/jcs.238337

Vav1-binding protein. Consistent with this finding, the reciprocal substitution, W56F, was previously shown to cause a ∼6-fold reduction in the activity of the Vav1 DH-PH-C1 module towards Rac1 (Chrencik et al., 2008). This residue lies at the base of the β2/β3 region of Rho GTPases, which has been implicated in the binding of RhoA and the exclusion of Cdc42 by Vav3 (Movilla et al., 2001). However, existing crystal structures of Rac1 in complex with Vav1 display minimal contacts with the β2/β3 region of the GTPase (Chrencik et al., 2008; Rapley et al., 2008). Nevertheless, the β2/β3 region of Rac1, which is often exploited for the discrimination of Rho GTPases, is poised over the loop between the α4 and α5 helices of Vav1. This region is strictly conserved in Vav1 (314-RANN-317) and Vav3 (312-RANN-315), while Vav2 has maintained a divergent sequence at this position (317-KVQD-320). One possibility is that Rho GTPases may initially contact the GEF surface via this region, but subsequently tilt away from this interface as induced rearrangements of the switch I and switch II regions stabilize the nucleotide-free state. In any case, our findings emphasize the fact that our understanding of how the Vav GEFs select their substrates is incomplete and that further structural studies will be required to resolve such questions.

It is not immediately apparent how active Cdc42 inhibits TCR-induced Ca^{2+} responses, as Cdc42 is activated following TCR ligation and accumulates within immune synapses (Cannon et al., 2001). However, TCR-dependent Cdc42 activation proceeds in the absence of LAT, SLP-76, Nck and Vav1, and is instead regulated by PIX family Rho GEFs (Ku et al., 2001; Phee et al., 2005). These GEFs participate in a complex with the Cdc42 effector PAK1 and the integrin-associated protein paxillin. Thus, the Cdc42 activation that is induced upon TCR ligation may primarily occur in integrin-rich signaling domains. We suggest that active Cdc42 is not normally produced within TCR-induced SLP-76 microclusters, and that the replacement of Vav1 by Vav2 inhibits Ca^{2+} responses by interfering with local signaling events.

Finally, we note that the ability of Vav2 to enhance B cell receptor-induced Ca^{2+} elevations, even though it inhibits the analogous TCR-initiated responses, highlights the fact that the signaling pathways of T cells and of B cells are 'wired' in fundamentally different ways (Doody et al., 2000). In contrast to Vav1 in T cells, Vav2 cannot enhance the Ca^{2+} responses of B cells unless it retains its catalytic activity. The salient GTPase effector of Vav2 in B cell receptor-mediated Ca^{2+} entry remains unclear, as our findings demonstrate that Vav2 binds, and may also be able to activate, multiple Rho family GTPases, including Rac1, Rac2 and Cdc42. Nevertheless, our work suggests that the paralogous antigen receptor-initiated signaling complexes of T cells and B cells have evolved profoundly different roles for Cdc42. We suggest that this discrepancy may be reflect the role of Cdc42 in the phagocytosis of large particles, which may promote antigen processing and presentation in B cells, while the uptake of TCR ligands may be detrimental due to the relative scarcity of these ligands (Hoppe and Swanson, 2004; Mohammadi and Isberg, 2013). In conclusion, the distinctive scaffolding and catalytic properties of Vav1 and Vav2 provide the first explanation for the divergent behaviors of these proteins in T cells, suggest a rationale for the differential usage of these proteins by different cell types, and may offer opportunities for the selective inhibition of Vav isoforms by small-molecule inhibitors.

MATERIALS AND METHODS

Cell lines and transfections

Jurkat T cells were maintained in complete medium, corresponding to RPMI 1640 (GE Healthcare and Lonza) supplemented with 10% fetal bovine serum (FBS), 20 mM L-glutamine (Lonza) and 10 µg ml^{-1} ciprofloxacin, at 37°C and 5% CO_2, and are routinely checked for contamination. E6.1 Jurkat T cells were obtained from the ATCC. Vav1-deficient Jurkat cells (J.Vav1 cells) were a gift of Robert T. Abraham (Sanford Burnham Prebys Medical Discovery Institute, La Jolla, CA, USA) (Cao et al., 2002). J.Vav1 cells stably expressing TRT-tagged SLP-76 were created using methods described previously (Ophir et al., 2013). SLP-76-deficient Jurkat cells stably expressing YFP-tagged SLP-76, J14.SY cells, were described previously (Bunnell et al., 2006). All lines are routinely tested to confirm TCR expression and the absence of the expected proteins. Transfections were performed by combining 300 µl of Jurkat cells at 4×10^7 cells ml^{-1} with up to 30 µg of DNA in a 4 mm gap cuvette and delivering one 300 V, 10 ms pulse using a BTX ECM 830 square wave electroporator. Cells recovered overnight in complete medium.

Constructs and molecular biology

All fluorescent chimeras were generated in pEGFP-n1 (Clontech) backbones and expressed under the control of minimized EF1α or SRα promoters. Plasmid numbers are provided for all vectors obtained from Addgene. All Vav1 chimeras were created from existing templates and correspond to NP_005419.2 (Sylvain et al., 2011). All Vav2 chimeras were developed from a plasmid deposited by Joan Brugge (Addgene #14554) and correspond to the long isoform of Vav2, NP_001127870.1 (equivalent to P52735) (Moores et al., 2000). Vav3 chimeras were developed using a vector obtained from the DNASU Plasmid Repository (HsCD00301689) and correspond to NP_006104.4. Vav1, Vav2 and Vav3 are respectively joined to their C-terminal fluorescent protein tags via the sequences SRRAPPVAT, IPVAT and PPVAT. Vav and GTPase chimeras were generated using standard molecular techniques or by employing custom gBlock fragments (Integrated DNA Technologies) in conjunction with the Gibson Assembly Cloning Kit (New England BioLabs) (Gibson et al., 2009). Junctional information for all domain-swapped chimeras is provided in the schematics accompanying the figures. mRFP1 and TagRFP-Turbo were originally provided by Roger Y. Tsien (Department of Chemistry & Biochemistry, UCSD, San Diego, CA, USA) (Shaner et al., 2004, 2008). mCerulean3 was created in-house from the sequence developed by M. Rizzo (Markwardt et al., 2011). All Rho GTPases were of human origin. Constructs containing the brain-specific isoform of Cdc42 (Cdc42b; NP_426359.1), mCitrine-Cdc42b (Addgene #11392), mCitrine-Cdc42b.G12V (Addgene #11399) and mCitrine-Cdc42b.T17N (Addgene #11400), were developed by Joel Swanson (Hoppe and Swanson, 2004). Constructs encoding the common form of Cdc42 (Cdc42p; NP_001034891.1) were generated by altering the equivalent brain isoforms. Cdc42p.Q61L was created by site-directed mutagenesis. YFP-Rac1 (Addgene #11391), YFP-Rac1.Q61L (Addgene #11401), YFP-Rac1.T17N (Addgene #11395), YFP-Rac2 (Addgene #11393) and YFP-Rac2.G12V (Addgene #11397), were also developed by Joel Swanson (Hoppe and Swanson, 2004). Wild-type EGFP-RhoA (Addgene #2965) and EGFP-RhoA.T19N (Addgene #12967) were developed by Gary Bokoch (Subauste et al., 2000). RhoG.G12V and RhoG.T17N were gifts of Ralph Isberg (Department of Molecular Biology & Microbiology, Tufts University Medical School, Boston, MA, USA) (Mohammadi and Isberg, 2009). All Rac1–Cdc42p chimeras were generated by standard cloning techniques after introducing silent restriction sites in regions conserved between Rac1 and Cdc42p.

Imaging

Cells imaged on glass-bottomed 96-well plates (Brooks Automation, Inc.) were prepared by activating with 0.01% poly-L-lysine, coating with 10 µg ml^{-1} OKT3 (anti-CD3ε) and blocking with 1% BSA as described previously (Bunnell et al., 2003). To image DN RhoG, anti-CD43 (BD Biosciences, clone 1G10) was added as described previously (Nguyen et al., 2008). For fixed cell imaging, cells were injected into wells in complete medium, incubated for 7 min at 37°C and 5% CO_2, fixed with 1% paraformaldehyde for 25 min at 37°C, then rinsed into PBS. Live-cell imaging was performed at 37°C in complete medium buffered with 25 mM HEPES pH 7.4. Cells were imaged continuously for 5 min shortly after landing and spreading. Image acquisition was performed using a spinning-disc confocal microscope, consisting of a 40× Plan-Neofluar oil immersion

objective lens (NA 1.3; Carl Zeiss), a 2.5× expanding lens, a spinning-disc confocal head (CSU-10; Yokogawa Corporation of America) and an Axiovert 200M stand (Carl Zeiss). All images were collected using an intensified CCD (ICCD) camera (XR MEGA-10; Stanford Photonics).

Image processing and quantification

Images were acquired using NIH-funded open-source Micro-Manager (Edelstein et al., 2010). Movies and kymographs were processed with iVision software (BioVision Technologies) as described previously (Sylvain et al., 2011; Ophir et al., 2013). Fixed image analysis was performed using NIH ImageJ and Fiji (Schindelin et al., 2012; Schneider et al., 2012). Automated cluster identification was performed using the version 1.01 GDSC plugin FindFoci (Herbert et al., 2014). Colocalization was quantified by using the GDSC match calculator to determine the fraction of clusters in the SLP-76–YFP channel that overlap, or occur within 300 nm of, clusters in the TRT–GTPase channel. Numbers reported here are the 'F1' output of the plugin: a weighted average of the fraction of colocalized clusters, specifically: 2/[(1/R1)+(1/R2)], where R1 is the fraction of points in RFP that also occur in YFP, and R2 is the fraction of points in YFP that also occur in RFP. F1 values for each condition were averaged across cells, and are presented as boxes enclosing the 2nd–3rd quartiles. Whiskers encompass the minimum and maximum observed values.

Ca^{2+} influx assays and analysis

Ca^{2+} influx assays were performed as described previously (Sylvain et al., 2011). Cells at 10^7 cells ml^{-1} were labeled with 10 µM Indo-1 AM (Life Technologies) for 1 h at 37°C, washed, resuspended at 10^6 cells ml^{-1} and kept on ice. Cells were equilibrated at 37°C before reading and maintained at 37°C throughout the assay. Ca^{2+} levels were monitored on an LSR II flow cytometer (BD Biosciences) using the ratio of Ca^{2+}-free Indo-1 emission (405/30 nm bandpass filter) to Ca^{2+}-bound Indo-1 emission (505 nm long-pass filter, 525/50 nm bandpass) upon excitation at 355 nm. Baseline readings were collected for 2 min, then cells were stimulated with 30 ng ml^{-1} OKT3 and monitored for an additional 10 min. For the Cdc42 inhibitor Ca^{2+} assays, cells were prepared as above, read for 60 s, brought to 100 µM of ZCL278 by adding 2 µl of 50 mM ZCL278 (ApexBio) (Friesland et al., 2013) in DMSO, or 2 µl of DMSO alone, then monitored for 5 min, stimulated with OKT3 and monitored for an additional 6 min. Data was analyzed using FlowJo software (Flowjo, LLC, version 8.8.7) by gating on null, medium and high expression of the transfected construct, and exporting the kinetic data to Microsoft Excel. For each of the three populations present within a single sample, the raw area under the curve (AUC) was calculated for the period of stimulation. The raw AUC was corrected by subtracting a hypothetical AUC calculated using the average pre-stimulation baseline. The percentage change is calculated by taking the corrected AUC of the low or high expressors, subtracting the AUC of the corresponding null expressors, and dividing by the AUC of the null expressors. Graphs show the mean±s.e.m.

The *P* values were computed using an unpaired, equal variance, two tailed, Student's *t*-test in Excel.

Relevant statistical considerations

Definition of sample size

For the Ca^{2+} assays, each experimental replicate involved an independent transfection. Statistical comparisons were performed using the number of experiments. Based on previous work, perturbations above the basal J.Vav1 response, via reconstitution with Vav1.WT, yield Cohen's effect sizes >10 in the high mYFP population and >5 in the low mYFP population. Perturbations below the basal J.Vav1 response, via reconstitution with Vav1.ΔCH, yield effect sizes >10 in the high mYFP population and >2 in the low mYFP population (Sylvain et al., 2011). Under these conditions n=3 is sufficient to incorrectly reject the null hypothesis <5% of the time, with a power of 90%. Comparable post-hoc effect sizes were observed here.

Inclusion and exclusion criteria

Pre-established inclusion criteria require that cell lines test as >70% CD3ε positive within 2 weeks of use. Ca^{2+} data were only excluded if positive controls performed at the beginning or end of session failed, indicating the presence of a technical defect. Statistical analyses of colocalization data were only performed for experiments conducted on the same instrument, using the same tagging schema, with the Vav chimera tagged with mCer3, the SLP-76 chimera tagged with mYFP and the GTPase tagged with TRT.

Appropriateness of statistical tests

Ca^{2+} samples were compared using a two-tailed Student's *t*-test for unpaired samples. Ca^{2+} data were normally distributed.

Antibodies and western blotting

Cells were stimulated with OKT3 (anti-CD3ε, BioExpress). Western blotting was performed by lysing cells in 50 mM Tris-HCl pH 8.0, 150 mM NaCl, 2 mM tetrasodium EDTA, 1% Triton X-100, 10 mM NaF, 1 mM Na_3VO_4, Complete protease inhibitor cocktail (Roche), 25 µg ml^{-1} Pepstatin A and 1 mM DTT. Lysates were boiled with sample buffer, run on 4–12% Bis-Tris Protein Gels (Life Technologies) and transferred to PVDF membranes. Membranes were blocked with 1% BSA and blotted with antibodies specific for GFP (JL-8, Clontech, 1:2000), Vav1 (07-192, EMD Millipore, 1:1000), Vav2 (ab52640, Abcam, 1:10,000), Vav3 (ab52938, Abcam, 1:5000), Cdc42 (2466, Cell Signaling Technology, 1:1000), Rac1 (ARC03, Cytoskeleton, 1:500) or Erk1/2 (4695, Cell Signaling Technology, 1:2000) primary antibodies. Horseradish peroxidase-conjugated anti-mouse-IgG (31432, Thermo Fisher Scientific, 1:10,000) and anti-rabbit-IgG (31462, Thermo Fisher Scientific, 1:10,000) were used as secondary antibodies, and western blots were developed by chemiluminescence (Super Signal; Thermo Fisher Scientific).

Databases

The expression data used in Fig. S2B to address the relative expression of Cdc42 splice isoforms in spleen and brain were acquired from Ensembl release 80 (Flicek et al., 2014).

Acknowledgements

We thank Allen Parmelee and Stephen Kwok of the Tufts Laser Cytometry facility for their assistance with cell sorting. We acknowledge the W.M. Keck Foundation and the Eshe Fund for their support of core facilities at Tufts.

Competing interests

The authors declare no competing or financial interests.

Author contributions

Conceptualization: M.A.F., J.C.C., N.R.S., S.C.B.; Methodology: M.A.F., N.R.S., M.-C.S., S.C.B.; Software: M.A.F., N.R.S., S.C.B.; Validation: M.A.F., J.C.C., N.R.S., S.C.B.; Formal analysis: M.A.F., J.C.C., N.R.S., S.C.B.; Investigation: M.A.F., J.C.C., N.R.S., M.-C.S.; Data curation: M.A.F., J.C.C., N.R.S., S.C.B.; Writing - original draft: M.A.F., N.R.S.; Writing - review & editing: M.A.F., J.C.C., N.R.S., M.-C.S., S.C.B.; Visualization: M.A.F., J.C.C., N.R.S., S.C.B.; Supervision: M.A.F., M.-C.S., S.C.B.; Project administration: S.C.B.; Funding acquisition: S.C.B.

Funding

This work was supported by funding from the American Heart Association (Scientist Development Grant 0635546T) and the National Institutes of Health (R01 AI076575-01). J.C.C. was supported by the National Institutes of Health (R25 GM076321), M.A.F. and N.R.S. also received support from the National Institutes of Health (T32 AI07077). Deposited in PMC for release after 12 months.

Supplementary information

Supplementary information available online at
http://jcs.biologists.org/lookup/doi/10.1242/jcs.238337.supplemental

Peer review history

The peer review history is available online at
https://jcs.biologists.org/lookup/doi/10.1242/jcs.238337.reviewer-comments.pdf

References

Abate, F., Da Silva-Almeida, A. C., Zairis, S., Robles-Valero, J., Couronne, L., Khiabanian, H., Quinn, S. A., Kim, M.-Y., Laginestra, M. A., Kim, C. et al. (2017). Activating mutations and translocations in the guanine exchange factor

VAV1 in peripheral T-cell lymphomas. *Proc. Natl. Acad. Sci. USA* **114**, 764-769. doi:10.1073/pnas.1608839114

Abe, K., Rossman, K. L., Liu, B., Ritola, K. D., Chiang, D., Campbell, S. L., Burridge, K. and Der, C. J. (2000). Vav2 is an activator of Cdc42, Rac1, and RhoA. *J. Biol. Chem.* **275**, 10141-10149. doi:10.1074/jbc.275.14.10141

Aghazadeh, B., Lowry, W. E., Huang, X.-Y. and Rosen, M. K. (2000). Structural basis for relief of autoinhibition of the Dbl homology domain of proto-oncogene Vav by tyrosine phosphorylation. *Cell* **102**, 625-633. doi:10.1016/S0092-8674(00)00085-4

Anderson, E. L. and Hamann, M. J. (2012). Detection of Rho GEF and GAP activity through a sensitive split luciferase assay system. *Biochem. J.* **441**, 869-879. doi:10.1042/BJ20111111

Arthur, W. T., Quilliam, L. A. and Cooper, J. A. (2004). Rap1 promotes cell spreading by localizing Rac guanine nucleotide exchange factors. *J. Cell Biol.* **167**, 111-122. doi:10.1083/jcb.200404068

Baier, A., Ndoh, V. N. E., Lacy, P. and Eitzen, G. (2014). Rac1 and Rac2 control distinct events during antigen-stimulated mast cell exocytosis. *J. Leukoc. Biol.* **95**, 763-774. doi:10.1189/jlb.0513281

Barreira, M., Fabbiano, S., Couceiro, J. R., Torreira, E., Martinez-Torrecuadrada, J. L., Montoya, G., Llorca, O. and Bustelo, X. R. (2014). The C-terminal SH3 domain contributes to the intramolecular inhibition of Vav family proteins. *Sci. Signal.* **7**, ra35. doi:10.1126/scisignal.2004993

Barreira, M., Rodríguez-Fdez, S. and Bustelo, X. R. (2018). New insights into the Vav1 activation cycle in lymphocytes. *Cell. Signal.* **45**, 132-144. doi:10.1016/j.cellsig.2018.01.026

Billadeau, D. D., Mackie, S. M., Schoon, R. A. and Leibson, P. J. (2000). Specific subdomains of Vav differentially affect T cell and NK cell activation. *J. Immunol.* **164**, 3971-3981. doi:10.4049/jimmunol.164.8.3971

Booden, M. A., Campbell, S. L. and Der, C. J. (2002). Critical but distinct roles for the pleckstrin homology and cysteine-rich domains as positive modulators of Vav2 signaling and transformation. *Mol. Cell. Biol.* **22**, 2487-2497. doi:10.1128/MCB.22.8.2487-2497.2002

Bunnell, S. C. (2010). Multiple microclusters: diverse compartments within the immune synapse. *Curr. Top. Microbiol. Immunol.* **340**, 123-154. doi:10.1007/978-3-642-03858-7_7

Bunnell, S. C., Hong, D. I., Kardon, J. R., Yamazaki, T., Mcglade, C. J., Barr, V. A. and Samelson, L. E. (2002). T cell receptor ligation induces the formation of dynamically regulated signaling assemblies. *J. Cell Biol.* **158**, 1263-1275. doi:10.1083/jcb.200203043

Bunnell, S. C., Barr, V. A., Fuller, C. L. and Samelson, L. E. (2003). High-resolution multicolor imaging of dynamic signaling complexes in T cells stimulated by planar substrates. *Sci. Signal.* **2003**, PL8. doi:10.1126/stke.2003.177.pl8

Bunnell, S. C., Singer, A. L., Hong, D. I., Jacque, B. H., Jordan, M. S., Seminario, M.-C., Barr, V. A., Koretzky, G. A. and Samelson, L. E. (2006). Persistence of cooperatively stabilized signaling clusters drives T-cell activation. *Mol. Cell. Biol.* **26**, 7155-7166. doi:10.1128/MCB.00507-06

Bustelo, X. R. (2012). Vav family. In *Encyclopedia of Signaling Molecules* (ed. S. Choi), pp. 1963-1977. New York, NY: Springer New York.

Bustelo, X. R. (2014). Vav family exchange factors: an integrated regulatory and functional view. *Small GTPases* **5**, 9. doi:10.4161/21541248.2014.973757

Cannon, J. L., Labno, C. M., Bosco, G., Seth, A., McGavin, M. H. K., Siminovitch, K. A., Rosen, M. K. and Burkhardt, J. K. (2001). Wasp recruitment to the T cell: APC contact site occurs independently of Cdc42 activation. *Immunity* **15**, 249-259. doi:10.1016/S1074-7613(01)00178-9

Cao, Y., Janssen, E. M., Duncan, A. W., Altman, A., Billadeau, D. D. and Abraham, R. T. (2002). Pleiotropic defects in TCR signaling in a Vav-1-null Jurkat T-cell line. *EMBO J.* **21**, 4809-4819. doi:10.1093/emboj/cdf499

Charvet, C., Canonigo, A. J., Billadeau, D. D. and Altman, A. (2005). Membrane localization and function of Vav3 in T cells depend on its association with the adapter SLP-76. *J. Biol. Chem.* **280**, 15289-15299. doi:10.1074/jbc.M500275200

Chrencik, J. E., Brooun, A., Zhang, H., Mathews, I. I., Hura, G. L., Foster, S. A., Perry, J. J. P., Streiff, M., Ramage, P., Widmer, H. et al. (2008). Structural basis of guanine nucleotide exchange mediated by the T-cell essential Vav1. *J. Mol. Biol.* **380**, 828-843. doi:10.1016/j.jmb.2008.05.024

Croker, B. A., Tarlinton, D. M., Cluse, L. A., Tuxen, A. J., Light, A., Yang, F.-C., Williams, D. A. and Roberts, A. W. (2002). The Rac2 guanosine triphosphatase regulates B lymphocyte antigen receptor responses and chemotaxis and is required for establishment of B-1a and marginal zone B lymphocytes. *J. Immunol.* **168**, 3376-3386. doi:10.4049/jimmunol.168.7.3376

Doody, G. M., Billadeau, D. D., Clayton, E., Hutchings, A., Berland, R., Mcadam, S., Leibson, P. J. and Turner, M. (2000). Vav-2 controls NFAT-dependent transcription in B- but not T-lymphocytes. *EMBO J.* **19**, 6173-6184. doi:10.1093/emboj/19.22.6173

Edelstein, A., Amodaj, N., Hoover, K., Vale, R. and Stuurman, N. (2010). Computer control of microscopes using μManager. *Curr. Protoc. Mol. Biol.* **92**, 14.20.1-14.20.17. doi:10.1002/0471142727.mb1420s92

Erickson, J. W., Zhang, C.-J., Kahn, R. A., Evans, T. and Cerione, R. A. (1996). Mammalian Cdc42 is a brefeldin A-sensitive component of the Golgi apparatus. *J. Biol. Chem.* **271**, 26850-26854. doi:10.1074/jbc.271.43.26850

Feig, L. A. (1999). Tools of the trade: use of dominant-inhibitory mutants of Ras-family GTPases. *Nat. Cell Biol.* **1**, E25-E27. doi:10.1038/10018

Fischer, K.-D., Zmuldzinas, A., Gardner, S., Barbacid, M., Bernstein, A. and Guidos, C. (1995). Defective T-cell receptor signalling and positive selection of Vav-deficient CD4+ CD8+ thymocytes. *Nature* **374**, 474-477. doi:10.1038/374474a0

Flajnik, M. F. and Kasahara, M. (2010). Origin and evolution of the adaptive immune system: genetic events and selective pressures. *Nat. Rev. Genet.* **11**, 47-59. doi:10.1038/nrg2703

Flicek, P., Amode, M. R., Barrell, D., Beal, K., Billis, K., Brent, S., Carvalho-Silva, D., Clapham, P., Coates, G., Fitzgerald, S. et al. (2014). Ensembl 2014. *Nucleic Acids Res.* **42**, D749-D755. doi:10.1093/nar/gkt1196

Friesland, A., Zhao, Y., Chen, Y.-H., Wang, L., Zhou, H. and Lu, Q. (2013). Small molecule targeting Cdc42-intersectin interaction disrupts Golgi organization and suppresses cell motility. *Proc. Natl. Acad. Sci. USA* **110**, 1261-1266. doi:10.1073/pnas.1116051110

Fujikawa, K., Miletic, A. V., Alt, F. W., Faccio, R., Brown, T., Hoog, J., Fredericks, J., Nishi, S., Mildiner, S., Moores, S. L. et al. (2003). Vav1/2/3-null mice define an essential role for Vav family proteins in lymphocyte development and activation but a differential requirement in MAPK signaling in T and B cells. *J. Exp. Med.* **198**, 1595-1608. doi:10.1084/jem.20030874

Gibson, D. G., Young, L., Chuang, R.-Y., Venter, J. C., Hutchison, C. A., III and Smith, H. O. (2009). Enzymatic assembly of DNA molecules up to several hundred kilobases. *Nat. Methods* **6**, 343-345. doi:10.1038/nmeth.1318

Guilluy, C., Dubash, A. D. and García-Mata, R. (2011). Analysis of RhoA and Rho GEF activity in whole cells and the cell nucleus. *Nat. Protoc.* **6**, 2050-2060. doi:10.1038/nprot.2011.411

Hamann, M. J., Lubking, C. M., Luchini, D. N. and Billadeau, D. D. (2007). Asef2 functions as a Cdc42 exchange factor and is stimulated by the release of an autoinhibitory module from a concealed C-terminal activation element. *Mol. Cell. Biol.* **27**, 1380-1393. doi:10.1128/MCB.01608-06

Hanna, S., Miskolci, V., Cox, D. and Hodgson, L. (2014). A new genetically encoded single-chain biosensor for Cdc42 based on FRET, useful for live-cell imaging. *PLoS ONE* **9**, e96469. doi:10.1371/journal.pone.0096469

Heo, J., Thapar, R. and Campbell, S. L. (2005). Recognition and activation of Rho GTPases by Vav1 and Vav2 guanine nucleotide exchange factors. *Biochemistry* **44**, 6573-6585. doi:10.1021/bi047443q

Heo, W. D., Inoue, T., Park, W. S., Kim, M. L., Park, B. O., Wandless, T. J. and Meyer, T. (2006). PI(3,4,5)P3 and PI(4,5)P2 lipids target proteins with polybasic clusters to the plasma membrane. *Science* **314**, 1458-1461. doi:10.1126/science.1134389

Herbert, A. D., Carr, A. M. and Hoffmann, E. (2014). FindFoci: a focus detection algorithm with automated parameter training that closely matches human assignments, reduces human inconsistencies and increases speed of analysis. *PLoS ONE* **9**, e114749. doi:10.1371/journal.pone.0114749

Hoppe, A. D. and Swanson, J. A. (2004). Cdc42, Rac1, and Rac2 display distinct patterns of activation during phagocytosis. *Mol. Biol. Cell* **15**, 3509-3519. doi:10.1091/mbc.e03-11-0847

Jaiswal, M., Dvorsky, R. and Ahmadian, M. R. (2013). Deciphering the molecular and functional basis of Dbl family proteins: a novel systematic approach toward classification of selective activation of the Rho family proteins. *J. Biol. Chem.* **288**, 4486-4500. doi:10.1074/jbc.M112.429746

Katzav, S. (2007). Flesh and blood: the story of Vav1, a gene that signals in hematopoietic cells but can be transforming in human malignancies. *Cancer Lett.* **255**, 241-254. doi:10.1016/j.canlet.2007.04.015

Knyazhitsky, M., Moas, E., Shaginov, E., Luria, A. and Braiman, A. (2012). Vav1 oncogenic mutation inhibits T cell receptor-induced calcium mobilization through inhibition of phospholipase Cγ1 activation. *J. Biol. Chem.* **287**, 19725-19735. doi:10.1074/jbc.M111.309799

Kogure, Y. and Kataoka, K. (2017). Genetic alterations in adult T-cell leukemia/lymphoma. *Cancer Sci.* **108**, 1719-1725. doi:10.1111/cas.13303

Ksionda, O., Saveliev, A., Köchl, R., Rapley, J., Faroudi, M., Smith-Garvin, J. E., Wülfing, C., Rittinger, K., Carter, T. and Tybulewicz, V. L. J. (2012). Mechanism and function of Vav1 localisation in TCR signalling. *J. Cell Sci.* **125**, 5302-5314. doi:10.1242/jcs.105148

Ku, G. M., Yablonski, D., Manser, E., Lim, L. and Weiss, A. (2001). A PAK1-PIX-PKL complex is activated by the T-cell receptor independent of Nck, Slp-76 and LAT. *EMBO J.* **20**, 457-465. doi:10.1093/emboj/20.3.457

Kuhne, M. R., Ku, G. and Weiss, A. (2000). A guanine nucleotide exchange factor-independent function of Vav1 in transcriptional activation. *J. Biol. Chem.* **275**, 2185-2190. doi:10.1074/jbc.275.3.2185

Leonard, D. A., Evans, T., Hart, M., Cerione, R. A. and Manor, D. (1994). Investigation of the GTP-binding/GTPase cycle of Cdc42Hs using fluorescence spectroscopy. *Biochemistry* **33**, 12323-12328. doi:10.1021/bi00206a040

Li, S.-Y., Du, M.-J., Wan, Y.-J., Lan, B., Liu, Y.-H., Yang, Y., Zhang, C.-Z. and Cao, Y. J. (2013). The N-terminal 20-amino acid region of guanine nucleotide exchange factor Vav1 plays a distinguished role in T cell receptor-mediated calcium signaling. *J. Biol. Chem.* **288**, 3777-3785. doi:10.1074/jbc.M112.426221

Markwardt, M. L., Kremers, G.-J., Kraft, C. A., Ray, K., Cranfill, P. J. C., Wilson, K. A., Day, R. N., Wachter, R. M., Davidson, M. W. and Rizzo, M. A. (2011). An

improved cerulean fluorescent protein with enhanced brightness and reduced reversible photoswitching. *PLoS ONE* **6**, e17896. doi:10.1371/journal.pone.0017896

Martínez-Martín, N., Fernández-Arenas, E., Cemerski, S., Delgado, P., Turner, M., Heuser, J., Irvine, D. J., Huang, B., Bustelo, X. R., Shaw, A. et al. (2011). T cell receptor internalization from the immunological synapse is mediated by TC21 and RhoG GTPase-dependent phagocytosis. *Immunity* **35**, 208-222. doi:10.1016/j.immuni.2011.06.003

Miletic, A. V., Graham, D. B., Sakata-Sogawa, K., Hiroshima, M., Hamann, M. J., Cemerski, S., Kloeppel, T., Billadeau, D. D., Kanagawa, O., Tokunaga, M. et al. (2009). Vav links the T cell antigen receptor to the actin cytoskeleton and T cell activation independently of intrinsic Guanine nucleotide exchange activity. *PLoS ONE* **4**, e6599. doi:10.1371/journal.pone.0006599

Ming, W., Li, S., Billadeau, D. D., Quilliam, L. A. and Dinauer, M. C. (2007). The Rac effector p67phox regulates phagocyte NADPH oxidase by stimulating Vav1 guanine nucleotide exchange activity. *Mol. Cell. Biol.* **27**, 312-323. doi:10.1128/MCB.00985-06

Mitin, N., Betts, L., Yohe, M. E., Der, C. J., Sondek, J. and Rossman, K. L. (2007). Release of autoinhibition of ASEF by APC leads to CDC42 activation and tumor suppression. *Nat. Struct. Mol. Biol.* **14**, 814-823. doi:10.1038/nsmb1290

Mohammadi, S. and Isberg, R. R. (2009). Yersinia pseudotuberculosis virulence determinants invasin, YopE, and YopT modulate RhoG activity and localization. *Infect. Immun.* **77**, 4771-4782. doi:10.1128/IAI.00850-09

Mohammadi, S. and Isberg, R. R. (2013). Cdc42 interacts with the exocyst complex to promote phagocytosis. *J. Cell Biol.* **200**, 81-93. doi:10.1083/jcb.201204090

Moores, S. L., Selfors, L. M., Fredericks, J., Breit, T., Fujikawa, K., Alt, F. W., Brugge, J. S. and Swat, W. (2000). Vav family proteins couple to diverse cell surface receptors. *Mol. Cell. Biol.* **20**, 6364-6373. doi:10.1128/MCB.20.17.6364-6373.2000

Movilla, N., Dosil, M., Zheng, Y. and Bustelo, X. R. (2001). How Vav proteins discriminate the GTPases Rac1 and RhoA from Cdc42. *Oncogene* **20**, 8057-8065. doi:10.1038/sj.onc.1205000

Nguyen, K., Sylvain, N. R. and Bunnell, S. C. (2008). T cell costimulation via the integrin VLA-4 inhibits the actin-dependent centralization of signaling microclusters containing the adaptor SLP-76. *Immunity* **28**, 810-821. doi:10.1016/j.immuni.2008.04.019

Nishimura, A. and Linder, M. E. (2013). Identification of a novel prenyl and palmitoyl modification at the CaaX motif of Cdc42 that regulates RhoGDI binding. *Mol. Cell. Biol.* **33**, 1417-1429. doi:10.1128/MCB.01398-12

Olenik, C., Aktories, K. and Meyer, D. K. (1999). Differential expression of the small GTP-binding proteins RhoA, RhoB, Cdc42u and Cdc42b in developing rat neocortex. *Brain Res. Mol. Brain Res.* **70**, 9-17. doi:10.1016/S0169-328X(99)00121-7

Ophir, M. J., Liu, B. C. and Bunnell, S. C. (2013). The N terminus of SKAP55 enables T cell adhesion to TCR and integrin ligands via distinct mechanisms. *J. Cell Biol.* **203**, 1021-1041. doi:10.1083/jcb.201305088

Phee, H., Abraham, R. T. and Weiss, A. (2005). Dynamic recruitment of PAK1 to the immunological synapse is mediated by PIX independently of SLP-76 and Vav1. *Nat. Immunol.* **6**, 608-617. doi:10.1038/ni1199

Prisco, A., Vanes, L., Ruf, S., Trigueros, C. and Tybulewicz, V. L. J. (2005). Lineage-specific requirement for the PH domain of Vav1 in the activation of CD4+ but not CD8+ T cells. *Immunity* **23**, 263-274. doi:10.1016/j.immuni.2005.07.007

Rapley, J., Tybulewicz, V. L. J. and Rittinger, K. (2008). Crucial structural role for the PH and C1 domains of the Vav1 exchange factor. *EMBO Rep.* **9**, 655-661. doi:10.1038/embor.2008.80

Reynolds, L. F., Smyth, L. A., Norton, T., Freshney, N., Downward, J., Kioussis, D. and Tybulewicz, V. L. J. (2002). Vav1 transduces T cell receptor signals to the activation of phospholipase C-γ1 via phosphoinositide 3-kinase-dependent and -independent pathways. *J. Exp. Med.* **195**, 1103-1114. doi:10.1084/jem.20011663

Rodríguez-Fdez, S., Citterio, C., Lorenzo-Martín, L. F., Baltanás-Copado, J., Llorente-González, C., Corbalán-García, S., Vicente-Manzanares, M. and Bustelo, X. R. (2019). Phosphatidylinositol monophosphates regulate optimal Vav1 signaling output. *Cells* **8**, 1649. doi:10.3390/cells8121649

Saveliev, A., Vanes, L., Ksionda, O., Rapley, J., Smerdon, S. J., Rittinger, K. and Tybulewicz, V. L. J. (2009). Function of the nucleotide exchange activity of vav1 in T cell development and activation. *Sci. Signal.* **2**, ra83. doi:10.1126/scisignal.2000420

Schindelin, J., Arganda-Carreras, I., Frise, E., Kaynig, V., Longair, M., Pietzsch, T., Preibisch, S., Rueden, C., Saalfeld, S., Schmid, B. et al. (2012). Fiji: an open-source platform for biological-image analysis. *Nat. Methods* **9**, 676-682. doi:10.1038/nmeth.2019

Schneider, C. A., Rasband, W. S. and Eliceiri, K. W. (2012). NIH Image to ImageJ: 25 years of image analysis. *Nat. Methods* **9**, 671-675. doi:10.1038/nmeth.2089

Schuebel, K. E., Movilla, N., Rosa, J. L. and Bustelo, X. R. (1998). Phosphorylation-dependent and constitutive activation of Rho proteins by wild-type and oncogenic Vav-2. *EMBO J.* **17**, 6608-6621. doi:10.1093/emboj/17.22.6608

Shaner, N. C., Campbell, R. E., Steinbach, P. A., Giepmans, B. N. G., Palmer, A. E. and Tsien, R. Y. (2004). Improved monomeric red, orange and yellow fluorescent proteins derived from Discosoma sp. red fluorescent protein. *Nat. Biotechnol.* **22**, 1567-1572. doi:10.1038/nbt1037

Shaner, N. C., Lin, M. Z., Mckeown, M. R., Steinbach, P. A., Hazelwood, K. L., Davidson, M. W. and Tsien, R. Y. (2008). Improving the photostability of bright monomeric orange and red fluorescent proteins. *Nat. Methods* **5**, 545-551. doi:10.1038/nmeth.1209

Shutes, A., Onesto, C., Picard, V., Leblond, B., Schweighoffer, F. and Der, C. J. (2007). Specificity and mechanism of action of EHT 1864, a novel small molecule inhibitor of Rac family small GTPases. *J. Biol. Chem.* **282**, 35666-35678. doi:10.1074/jbc.M703571200

Subauste, M. C., Von Herrath, M., Benard, V., Chamberlain, C. E., Chuang, T.-H., Chu, K., Bokoch, G. M. and Hahn, K. M. (2000). Rho family proteins modulate rapid apoptosis induced by cytotoxic T lymphocytes and Fas. *J. Biol. Chem.* **275**, 9725-9733. doi:10.1074/jbc.275.13.9725

Sylvain, N. R., Nguyen, K. and Bunnell, S. C. (2011). Vav1-mediated scaffolding interactions stabilize SLP-76 microclusters and contribute to antigen-dependent T cell responses. *Sci. Signal.* **4**, ra14. doi:10.1126/scisignal.2001178

Tartare-Deckert, S., Monthouel, M.-N., Charvet, C., Foucault, I., Van Obberghen, E., Bernard, A., Altman, A. and Deckert, M. (2001). Vav2 activates c-fos serum response element and CD69 expression but negatively regulates nuclear factor of activated T cells and interleukin-2 gene activation in T lymphocyte. *J. Biol. Chem.* **276**, 20849-20857. doi:10.1074/jbc.M010588200

Tedford, K., Nitschke, L., Girkontaite, I., Charlesworth, A., Chan, G., Sakk, V., Barbacid, M. and Fischer, K.-D. (2001). Compensation between Vav-1 and Vav-2 in B cell development and antigen receptor signaling. *Nat. Immunol.* **2**, 548-555. doi:10.1038/88756

Turner, M. and Billadeau, D. D. (2002). VAV proteins as signal integrators for multi-subunit immune-recognition receptors. *Nat. Rev. Immunol.* **2**, 476-486. doi:10.1038/nri840

Turner, M., Mee, P. J., Walters, A. E., Quinn, M. E., Mellor, A. L., Zamoyska, R. and Tybulewicz, V. L. J. (1997). A requirement for the Rho-family GTP exchange factor Vav in positive and negative selection of thymocytes. *Immunity* **7**, 451-460. doi:10.1016/S1074-7613(00)80367-2

Wirth, A., Chen-Wacker, C., Wu, Y.-W., Gorinski, N., Filippov, M. A., Pandey, G. and Ponimaskin, E. (2013). Dual lipidation of the brain-specific Cdc42 isoform regulates its functional properties. *Biochem. J.* **456**, 311-322. doi:10.1042/BJ20130788

Wu, J., Katzav, S. and Weiss, A. (1995). A functional T-cell receptor signaling pathway is required for p95vav activity. *Mol. Cell. Biol.* **15**, 4337-4346. doi:10.1128/MCB.15.8.4337

Yu, H., Leitenberg, D., Li, B. and Flavell, R. A. (2001). Deficiency of small GTPase Rac2 affects T cell activation. *J. Exp. Med.* **194**, 915-926. doi:10.1084/jem.194.7.915

Yu, B., Martins, I. R. S., Li, P., Amarasinghe, G. K., Umetani, J., Fernandez-Zapico, M. E., Billadeau, D. D., Machius, M., Tomchick, D. R. and Rosen, M. K. (2010). Structural and energetic mechanisms of cooperative autoinhibition and activation of Vav1. *Cell* **140**, 246-256. doi:10.1016/j.cell.2009.12.033

Zakaria, S., Gomez, T. S., Savoy, D. N., Mcadam, S., Turner, M., Abraham, R. T. and Billadeau, D. D. (2004). Differential regulation of TCR-mediated gene transcription by Vav family members. *J. Exp. Med.* **199**, 429-434. doi:10.1084/jem.20031228

Zhou, Z., Yin, J., Dou, Z., Tang, J., Zhang, C. and Cao, Y. (2007). The calponin homology domain of Vav1 associates with calmodulin and is prerequisite to T cell antigen receptor-induced calcium release in Jurkat T lymphocytes. *J. Biol. Chem.* **282**, 23737-23744. doi:10.1074/jbc.M702975200

Zugaza, J. L., López-Lago, M. A., Caloca, M. J., Dosil, M., Movilla, N. and Bustelo, X. R. (2002). Structural determinants for the biological activity of Vav proteins. *J. Biol. Chem.* **277**, 45377-45392. doi:10.1074/jbc.M208039200